

Measurements of  
nitrogen oxides and  
ozone fluxes

P. Stella et al.

# Measurements of nitrogen oxides and ozone fluxes by eddy covariance at a meadow: evidence for an internal leaf resistance to NO<sub>2</sub>

P. Stella<sup>1</sup>, M. Kortner<sup>1,\*</sup>, C. Ammann<sup>2</sup>, T. Foken<sup>3,4</sup>, F. X. Meixner<sup>1</sup>, and I. Trebs<sup>1</sup>

<sup>1</sup>Max Planck Institute for Chemistry, Biogeochemistry Department, 55020 Mainz, Germany

<sup>2</sup>Agroscope ART, Air Pollution and Climate Group, 8046 Zürich, Switzerland

<sup>3</sup>University of Bayreuth, Department of Micrometeorology, 95440 Bayreuth, Germany

<sup>4</sup>Member of Bayreuth Center of Ecology and Environmental Research (BayCEER), Germany

\* now at: Müller-BBM GmbH, Branch Office Frankfurt, 63589 Linsengericht, Germany

Received: 30 January 2013 – Accepted: 17 February 2013 – Published: 7 March 2013

Correspondence to: P. Stella (patrick.stella@mpic.de)

Published by Copernicus Publications on behalf of the European Geosciences Union.

Title Page

Abstract

Introduction

Conclusions

References

Tables

Figures



Back

Close

Full Screen / Esc

Printer-friendly Version

Interactive Discussion



## Abstract

Nitrogen dioxide (NO<sub>2</sub>) plays an important role in atmospheric pollution, in particular for tropospheric ozone production. However, the removal processes involved in NO<sub>2</sub> deposition to terrestrial ecosystems are still subject of ongoing discussion. This study reports NO<sub>2</sub> flux measurements made over a meadow using the eddy covariance method. The measured NO<sub>2</sub> deposition fluxes during daytime were about a factor of two lower than a priori calculated fluxes using the Surfalm model without taking into account an internal (also called mesophyllic or sub-stomatal) resistance. Neither an underestimation of the measured NO<sub>2</sub> deposition flux due to chemical divergence or direct NO<sub>2</sub> emission, nor an underestimation of the resistances used to model the NO<sub>2</sub> deposition explained the large difference between measured and modelled NO<sub>2</sub> fluxes. Thus, only the existence of the internal resistance could account for this large discrepancy between model and measurements. The median internal resistance was estimated to 300 sm<sup>-1</sup> during daytime, but exhibited a large variability (100 sm<sup>-1</sup> to 800 sm<sup>-1</sup>). In comparison, the stomatal resistance was only around 100 sm<sup>-1</sup> during daytime. Hence, the internal resistance accounted for 50 % to 90 % of the total leaf resistance to NO<sub>2</sub>. This study presents the first clear evidence and quantification of the internal resistance using the eddy covariance method, i.e. plant functioning was not affected by changes of microclimatological (turbulent) conditions that typically occur when using enclosure methods.

## 1 Introduction

Nitrogen oxides (NO<sub>x</sub>, the sum of nitric oxide, NO, and nitrogen dioxide, NO<sub>2</sub>) play an important role in the photochemistry of the atmosphere. By controlling the levels of key radical species such as the hydroxyl radical (OH), NO<sub>x</sub> are key compounds that influence the oxidative capacity of the atmosphere. In addition, NO<sub>x</sub> are closely linked with tropospheric ozone (O<sub>3</sub>) production. NO is rapidly oxidized to NO<sub>2</sub>, which is photo-

BGD

10, 4461–4514, 2013

## Measurements of nitrogen oxides and ozone fluxes

P. Stella et al.

Title Page

Abstract

Introduction

Conclusions

References

Tables

Figures

⏪

⏩

◀

▶

Back

Close

Full Screen / Esc

Printer-friendly Version

Interactive Discussion



## Measurements of nitrogen oxides and ozone fluxes

P. Stella et al.

[Title Page](#)

[Abstract](#)

[Introduction](#)

[Conclusions](#)

[References](#)

[Tables](#)

[Figures](#)

⏪

⏩

◀

▶

[Back](#)

[Close](#)

[Full Screen / Esc](#)

[Printer-friendly Version](#)

[Interactive Discussion](#)



dissociated to NO and ground-state atomic oxygen ( $O(^3P)$ ) that reacts with  $O_2$  to form  $O_3$  (Crutzen, 1970, 1979).  $O_3$  is a well known greenhouse gas responsible for positive radiative forcing, i.e. contributing to global warming, representing 25 % of the net radiative forcing attributed to human activities since the beginning of the industrial era. Moreover, due to its oxidative capacities,  $O_3$  is also a harmful pollutant responsible for damages on materials (Almeida et al., 2000; Boyce et al., 2001), human health (Levy et al., 2005; Hazucha and Lefohn, 2007) and plants (Paoletti, 2005; Ainsworth, 2008). In natural environments,  $O_3$  may lead to biodiversity losses, while in agro-ecosystems, it induces crop yield losses (Hillstrom and Lindroth, 2008; Avnery et al., 2011a,b; Payne et al., 2011).

$NO_x$  is also responsible for the production of nitric acid and organic nitrates, both acid rain and aerosol precursors (Crutzen, 1983). In addition, it influences the formation of nitrous acid (HONO), which is an important precursor for OH radicals in the atmosphere.

The important impacts of NO,  $NO_2$  and  $O_3$  on both atmospheric chemistry and environmental pollution require to establish the atmospheric budgets of these gases. Therefore, it is necessary (i) to identify the different sources and sinks of NO,  $NO_2$  and  $O_3$ , and (ii) to understand the processes governing the exchange of these compounds between the atmosphere and the biosphere. To achieve this goal, several studies were carried out in the last decades over various ecosystems to identify the underlying processes controlling the biosphere-atmosphere exchanges of NO (e.g. Meixner, 1994; Meixner et al., 1997; Ludwig et al., 2001; Laville et al., 2009; Bargsten et al., 2010),  $NO_2$  (e.g. Meixner, 1994; Eugster and Hesterberg, 1996; Hereid and Monson, 2001; Chaparro-Suarez et al., 2011; Breuninger et al., 2012), and  $O_3$  (e.g. Zhang et al., 2002; Rummel et al., 2007; Stella et al., 2011a).

It is now well established that soil biogenic NO emission depends on several factors, such as the amount of soil moisture, soil temperature, and soil nitrogen (Remde et al., 1989; Remde and Conrad, 1991; Ludwig et al., 2001; Laville et al., 2009). Ozone is deposited to terrestrial ecosystems through dry deposition (Fowler et al., 2009). The

different O<sub>3</sub> deposition pathways are well identified and the variables controlling each pathway are well understood: the cuticular and soil ozone deposition pathways are governed by canopy structure (canopy height, leaf area index) and relative humidity at the leaf and soil surface (Zhang et al., 2002; Altimir et al., 2006; Lamaud et al., 2009; Stella et al., 2011a), while stomatal ozone flux is controlled by climatic variables responsible for stomata opening such as radiation, temperature and vapour pressure deficit (Emberson et al., 2000; Gerosa et al., 2004).

However, the processes governing the NO<sub>2</sub> exchange between the atmosphere and the biosphere still remain unclear. While it is well recognized that NO<sub>2</sub> is mainly deposited through stomata, with the cuticular and soil fluxes being insignificant deposition pathways for NO<sub>2</sub> (Rondón et al., 1993; Segschneider et al., 1995; Pilegaard et al., 1998; Geßler et al., 2000; Ludwig et al., 2001), the existence of an internal resistance (also called mesophylllic or sub-stomatal resistance in previous studies) limiting NO<sub>2</sub> stomatal uptake is still under discussion. Previous studies reported contrasting results: Segschneider et al. (1995) and Geßler et al. (2000, 2002) did not find an internal resistance for sunflower, beech and spruce, whereas the results obtained by Sparks et al. (2001) and Teklemariam and Sparks (2006) for herbaceous plant species and tropical wet forest suggested its existence. In addition, the importance of this internal resistance for the overall NO<sub>2</sub> sink is not well established. Current estimates range from 3% to 60% of the total resistance to NO<sub>2</sub> uptake (Johansson, 1987; Gut et al., 2002; Chaparro-Suarez et al., 2011). Nevertheless, all the previous studies explored the processes of NO<sub>2</sub> exchange using enclosure (chamber) methods under field or controlled conditions, which may affect the microclimatological conditions around the plant leaves. This issue is of particular concern since the biochemical processes probably responsible for the internal resistance are linked with leaf functioning (Eller and Sparks, 2006; Hu and Sun, 2010). In addition, the aerodynamic resistance and the quasi-laminar boundary layer resistance above the plant leaves may be modified when applying enclosure methods.

## Measurements of nitrogen oxides and ozone fluxes

P. Stella et al.

Title Page

Abstract

Introduction

Conclusions

References

Tables

Figures

◀

▶

◀

▶

Back

Close

Full Screen / Esc

Printer-friendly Version

Interactive Discussion



## Measurements of nitrogen oxides and ozone fluxes

P. Stella et al.

Title Page

Abstract

Introduction

Conclusions

References

Tables

Figures

⏪

⏩

◀

▶

Back

Close

Full Screen / Esc

Printer-friendly Version

Interactive Discussion



In this study we present results of the SALSA campaign (SALSA: German acronym for “Contribution of nitrous acid (HONO) to the atmospheric OH-budget”, for details see Mayer et al., 2008). Turbulent fluxes of NO, NO<sub>2</sub> and O<sub>3</sub> were measured at a meadow below the Meteorological Observatory Hohenpeissenberg (MOHp) using the eddy covariance method. These measurements were accompanied by a comprehensive micrometeorological setup involving vertical profiles of trace gases and temperature as well as by eddy covariance measurements of carbon dioxide (CO<sub>2</sub>) and water vapor fluxes. In the present work, (i) the influence of chemical divergence was estimated above and within the canopy, (ii) the existence of an NO<sub>2</sub> compensation point mixing ratio was explored, (iii) the impact of the soil resistance to modeled NO<sub>2</sub> deposition was discussed and (iv) the internal resistance for NO<sub>2</sub> was quantified in order to understand the processes governing the NO<sub>2</sub> exchange.

## 2 Materials and methods

### 2.1 Site description

The field study was made at a meadow in the complex landscape around Hohenpeissenberg (Southern Germany) within the framework of the SALSA campaign (see Mayer et al., 2008; Trebs et al., 2009). The site consists in a managed and fertilized meadow located at the gentle lower (743 m a.s.l.) WSW-slope (3–4°) of the mountain Hoher Peißenberg (summit 988 m a.s.l.), directly west of the village Hohenpeissenberg in Bavaria, Southern Germany (coordinates: 47° 48′ N, 11° 02′ E). The surrounding pre-alpine landscape is characterized by its glacially shaped, hilly relief and a patchy land use dominated by the alternation of cattle pastures, meadows, mainly coniferous forests and rural settlements. The meadow is growing on clay-rich soil that can be classified as gley-colluvium with very small patches of marsh soil. Furthermore, it was characterized by its relatively low plant biodiversity and consisted mainly of perennial ryegrass (*Lolium perenne* L.), ribwort (*Plantago lanceolata* L.), dandelion (*Taraxacum*

*officinale*), red clover (*Trifolium pratense* L.), white clover (*Trifolium repens* L.), common cow parsnip (*Heracleum sphondylium* L.), sour dock (*Rumex acetosa* L.), daisy (*Bellis perennis* L.), and cow parsley (*Anthriscus sylvestris* (L.) Hoffm.).

The experiment was carried out from 29 August to 20 September 2005. The meadow was mown just before the instrument setup. The canopy height ( $h_c$ ) and leaf area index (LAI) increased from 15 cm and  $2.9 \text{ m}^2 \text{ m}^{-2}$  (at the beginning of the campaign) to 25 cm and  $4.9 \text{ m}^2 \text{ m}^{-2}$  at the end of the experiment, respectively. The roughness length ( $z_0 = 0.1 h_c$ ) ranged from 1.5 cm to 2.5 cm and the displacement height ( $d = 0.7 h_c$ ) varied between 10.5 cm and 17.5 cm. These values were confirmed by estimates of  $z_0$  and  $d$  from flux and profile records for 10 to 15 September.

The setup consisted of five measurement stations, (all located in an area of  $400 \text{ m}^2$ , with a distance of 20 to 30 m to each other). The stations recorded meteorological conditions (“MET 1” and “MET 2” from the Bayreuth University (UBT) and the Max Planck Institute for Chemistry (MPIC), respectively), mixing ratio profiles (“PROFILE” from the MPIC) and turbulent fluxes (“EC 1” and “EC 2” from the UBT and the MPIC, respectively) (see Table 1). The detailed measurement setups are described in Table 1 and the following sections.

## 2.2 Meteorological measurements

The following standard meteorological variables (and vertical profiles) were recorded: global radiation ( $G_r$ ) and net radiation, relative humidity (RH), air temperature ( $T_a$ ), wind speed ( $u$ ) and direction, and rainfall (for details see Table 1). The photolysis rate of  $\text{NO}_2$  ( $j_{\text{NO}_2}$ ), soil temperature ( $T_{\text{soil}}$ ) and soil water content (SWC) were also measured.

## 2.3 Trace gas profile measurements

Profile measurements of  $\text{NO}$ ,  $\text{O}_3$ , and  $\text{NO}_2$  mixing ratios were made in order to investigate the chemistry of the  $\text{NO-O}_3\text{-NO}_2$  triad above and within the canopy. The profile system consisted of six measurement levels: one inside the canopy (0.05 m

**BGD**

10, 4461–4514, 2013

## Measurements of nitrogen oxides and ozone fluxes

P. Stella et al.

Title Page

Abstract

Introduction

Conclusions

References

Tables

Figures

◀

▶

◀

▶

Back

Close

Full Screen / Esc

Printer-friendly Version

Interactive Discussion



**Measurements of  
nitrogen oxides and  
ozone fluxes**

P. Stella et al.

[Title Page](#)[Abstract](#)[Introduction](#)[Conclusions](#)[References](#)[Tables](#)[Figures](#)[⏪](#)[⏩](#)[◀](#)[▶](#)[Back](#)[Close](#)[Full Screen / Esc](#)[Printer-friendly Version](#)[Interactive Discussion](#)

a.g.l.), one at the canopy top (first in 0.20 m, later moved to 0.28 m), and four above the canopy (0.50 m, 1.00 m, 1.65 m and 3.00 m). The NO, O<sub>3</sub>, and NO<sub>2</sub> analyzers were located in an air conditioned container about 60 m north-east from the air inlets. The profile system was described previously by Mayer et al. (2011). Briefly, air samples from all heights were analyzed by the same analyzer consecutively and the levels were switched automatically by a valve system directly in front of a Teflon<sup>®</sup> diaphragm pump. The length of the opaque inlet lines made of PFA (perfluoroalkoxy copolymer) ranged from 62 to 65 m (depending on the sampling height). All non-active tubes were continuously flushed by a bypass pump. To avoid condensation of water vapor inside the tubes, they were insulated and heated to a few degrees above ambient temperature. Pressure and temperature in the tubes were monitored continuously. The individual heights were sampled with different frequencies: ambient air from the inlet levels at 0.50 m and 1.65 m were sampled ten times, other levels five times per 60 min (with each interval consisting of three individually recorded 30 s subintervals). Data from the first 30 s interval at each level were discarded to take into account the equilibration time of tubing and analyzers.

NO was measured by red-filtered detection of chemiluminescence – generated by the NO + O<sub>3</sub> reaction – with a CLD 780TR (EcoPhysics, Switzerland). Excess O<sub>3</sub> was frequently added in the pre-reaction chamber to account for interference of other trace gases. For the conversion of NO<sub>2</sub> to detectable NO, photolysis is the most specific technique (Kley and McFarland, 1980; Ridley et al., 1988). Thus, NO<sub>2</sub> in ambient air was photolytically converted to NO by directing every air sample air through a Blue Light converter (BLC, Droplet Measurement Technologies Inc.). Here, the light source was an UV diode array, which emits radiation within a very narrow spectral band (385–405 nm), making the NO<sub>2</sub> to NO conversion more specific and the conversion efficiency more stable in time than conventional converters based on photolysis of a broad spectral continuum (Pollack et al., 2011). The NO<sub>2</sub> mixing ratio can be determined from the difference between the NO mixing ratios measured with BLC and by-passing the BLC, respectively. The NO analyzer was calibrated by diluting a certified NO standard gas

(5.0 ppm, Air Liquide). The detection limit of the CLD 780TR was 90 ppt ( $3\sigma$ -definition). The efficiency of the photolytic conversion of  $\text{NO}_2$  to NO was determined by a back titration procedure involving the reaction of  $\text{O}_3$  with NO using a gas phase titration system (Dynamic Gas Calibrator 146 C, Thermo Environmental Instruments Inc., USA). Conversion efficiencies were about 33 %. Ozone mixing ratios of the ambient air samples were measured by an UV absorption instrument (49 C, Thermo Environment, USA).

## 2.4 Eddy covariance measurements

Eddy covariance has been extensively used during the last decades to estimate turbulent fluxes of momentum, heat and (non-reactive) trace gases (Running et al., 1999; Aubinet et al., 2000; Baldocchi et al., 2001; Dolman et al., 2006; Skiba et al., 2009). It is a direct measurement method to determine the exchange of mass and energy between the atmosphere and terrestrial surfaces without application of any empirical constant. The theoretical background for the eddy covariance can be found in existing literature (e.g. Foken, 2008; Foken et al., 2012; Aubinet et al., 2012) and will not be detailed here.

The turbulent fluxes of momentum ( $\tau$ ), sensible ( $H$ ) and latent heat (LE),  $\text{CO}_2$ , NO,  $\text{NO}_2$  and  $\text{O}_3$  were measured by two EC stations (Table 1). One station (MPIC) was dedicated to the measurement of NO- $\text{NO}_2$ - $\text{O}_3$  (as well as momentum and sensible heat,  $H$ ) fluxes, while the second (UBT), located  $\sim 20$  m in the southern direction, measured momentum,  $H$ , LE, and  $\text{CO}_2$  fluxes. The fetch was limited to around 50 m in the NW and NE sector, but extended at least to 150 m in all other directions. Three dimensional wind speed and temperature fluctuations were measured by sonic anemometers (Table 1) For high-frequency  $\text{CO}_2$  and water vapor measurements an open-path infrared gas analyzer (IRGA 7500, LiCor, USA) was used. High frequency (5 Hz) time series of NO and  $\text{NO}_2$  were determined with a fast-response and highly sensitive closed-path 2-channel chemiluminescence NO analyzer (CLD 790SR-2, EcoPhysics, Switzerland) coupled with a photolytic converter (Blue Light converter, BLC, Droplet Measurement Technologies Inc, USA) for the detection of  $\text{NO}_2$  (see Sect. 2.3). The NO detection

Title Page

Abstract

Introduction

Conclusions

References

Tables

Figures



Back

Close

Full Screen / Esc

Printer-friendly Version

Interactive Discussion



principle of the CLD 790SR-2 is identical to that of the CLD 780TR described above. However, the sensitivity is a factor of 10 higher than that of the CLD 780TR, and due to the presence of two channels the concentrations of NO and NO<sub>2</sub> can be measured simultaneously with high time resolution (see Hosaynali Beygi et al., 2011). The accuracy of the CLD790SR-2 is about 5 % and the NO detection limit for a one-second integration time is 10 ppt (3σ-definition). The instrument was also located in the air-conditioned container, about 60 m NE from the sonic anemometer. The trace gas inlets were fixed 33 cm below the sound path of the anemometer without horizontal separation at a three-pod mast. Air was sampled through two heated and opaque PFA tubes with a length of 63 m and an inner diameter of 4.4 mm. While the first sample line and CLD channel was used for measuring NO, a BLC converter was placed just behind the sample inlet of the second channel in a ventilated housing mounted at a boom of the measurement mast. Despite the low volume of the BLC (17 mL), conversion efficiencies γ for NO<sub>2</sub> to NO of around 41 % were achieved. Consequently this channel detected a partial NO<sub>x</sub> signal (denoted here as NO<sub>x</sub><sup>\*</sup>) corresponding to:

$$\chi\{\text{NO}_x^*\} = \chi\{\text{NO}\} + \gamma \cdot \chi\{\text{NO}_2\} \quad (1)$$

Flow restrictors for both channels of the CLD790SR-2 were mounted into the tubing closely after the corresponding inlets (after the BLC in the second channel) in order to achieve short residence times of the air samples inside the tubing (9 ± 0.4 s and 13 ± 0.4 s for NO and NO<sub>2</sub>, respectively) and fully turbulent conditions. The EC flux for the two analyzer channels were first calculated independently and the NO<sub>2</sub> flux was then determined as:

$$F_{\text{NO}_2} = \frac{1}{\gamma} \cdot (F_{\text{NO}_x^*} - F_{\text{NO}}) \quad (2)$$

Simultaneously, eddy covariance fluxes of O<sub>3</sub> were measured with a surface chemiluminescence instrument (Table 1) (Güsten et al., 1992; Güsten and Heinrich, 1996), which has been mounted on the three-pod mast with its inlet mounted directly next to that of NO and NO<sub>2</sub>.

**BGD**

10, 4461–4514, 2013

## Measurements of nitrogen oxides and ozone fluxes

P. Stella et al.

Title Page

Abstract

Introduction

Conclusions

References

Tables

Figures

◀

▶

◀

▶

Back

Close

Full Screen / Esc

Printer-friendly Version

Interactive Discussion



## Measurements of nitrogen oxides and ozone fluxes

P. Stella et al.

Title Page

Abstract

Introduction

Conclusions

References

Tables

Figures



Back

Close

Full Screen / Esc

Printer-friendly Version

Interactive Discussion



The 5 Hz signals of both CLD790SR-2 channels, referenced to the frequently calibrated NO and NO<sub>2</sub> measurements at 1.65 m from the trace gas profile system, were used for the final calculation of NO and NO<sub>2</sub> fluxes for 30 min time intervals. The O<sub>3</sub> flux calibration was done according to Muller et al. (2010). The quality of the derived fluxes was evaluated with the quality assessment schemes of Foken and Wichura (1996) (see also Foken et al., 2004), which validates the development state of turbulence by comparing the measured integral turbulence characteristics. Flux calculations included despiking of scalar time series (Vickers and Mahrt, 1997), planar fit coordinate rotation (Wilczak et al., 2001), linear detrending, correction of the time lag induced by the 63 m inlet tube, and correction for flux losses due to the attenuation of high frequency contributions according to Spirig et al. (2005) based on ogive analysis (Oncley, 1989; Desjardins et al., 1989). The high frequency losses were typically 12–20 % for NO, 16–25 % for NO<sub>2</sub> and 6–8 % for O<sub>3</sub>. Since pressure and temperature were held constant by the instruments and the effect of water vapor fluctuations was negligible, corrections for density fluctuations (WPL-corrections, Webb et al., 1980) were not necessary for NO, NO<sub>2</sub> and O<sub>3</sub>.

### 2.5 Resistance model parameterisations

The transfer of heat and trace gases can be assimilated into a resistance network with analogy to the Ohm's law (Wesely, 1989; Wesely and Hicks, 2000). It includes the turbulent resistance above ( $R_a$ ) and within ( $R_{ac}$ ) the canopy, the quasi-laminar boundary layer ( $R_b$ ), the stomatal ( $R_s$ ) and internal ( $R_{int}$ ) resistances, the cuticular resistance ( $R_{cut}$ ) and the soil resistance ( $R_{soil}$ ).

In order to investigate the processes governing the exchanges of NO<sub>2</sub> and O<sub>3</sub>, we used the Surfalm model developed to simulate exchanges of heat and pollutant between the atmosphere and the vegetation (Personne et al., 2009; Stella et al., 2011b). It is a multi-resistance Soil-Vegetation-Atmosphere-Transfer (SVAT) model which couples (i) a trace gas exchange model and (ii) an energy budget model allowing to estimate the temperature and humidity of the leaves and of the soil to calculate the resistances to

trace gas exchange. It comprises one vegetation layer and one soil layer. This model was initially developed to simulate the ammonia exchange and it was validated over grasslands by Personne et al. (2009), and recently adapted to estimate O<sub>3</sub> deposition to several maize crops by Stella et al. (2011b). In the following, we will only focus on the specific resistances to NO<sub>2</sub> and O<sub>3</sub> deposition. However, more details and explanations concerning the resistive scheme and the resistance parameterizations can be found in Personne et al. (2009) and Stella et al. (2011b).

The resistive scheme for NO<sub>2</sub> and O<sub>3</sub> deposition is shown in Fig. 1. Turbulent resistances above and within the canopy are identical for both NO<sub>2</sub> and O<sub>3</sub>, and were expressed as:

$$R_a(z_{\text{ref}}) = \frac{1}{k^2 \cdot u(z_{\text{ref}})} \cdot \left\{ \ln \left( \frac{z_{\text{ref}} - d}{z_{0T}} \right) - \Psi_H((z_{\text{ref}} - d)/L) \right\} \cdot \left\{ \ln \left( \frac{z_{\text{ref}} - d}{z_{0M}} \right) - \Psi_M((z_{\text{ref}} - d)/L) \right\} \quad (3)$$

$$R_{ac} = \frac{h_c \cdot \exp(\alpha_u)}{\alpha_u \cdot K_M(h_c)} \cdot \left\{ \exp \left( \frac{-\alpha_u \cdot z_{0s}}{h_c} \right) - \exp \left( \frac{-\alpha_u \cdot (d + z_{0M})}{h_c} \right) \right\} \quad (4)$$

where  $k$  ( $= 0.4$ ) is the von Kármán's constant,  $z_{\text{ref}}$  is the reference height,  $d$  is the displacement height,  $z_{0T}$  and  $z_{0M}$  are the canopy roughness length for temperature and momentum respectively,  $z_{0s}$  ( $= 0.02$  m; Personne et al., 2009) is the ground surface roughness length below the canopy,  $h_c$  is the canopy height,  $u(z_{\text{ref}})$  is the wind speed at  $z_{\text{ref}}$ ,  $\alpha_u$  ( $= 4.2$ ) is the attenuation coefficient for the decrease of the wind speed inside the canopy (Raupach et al., 1996),  $K_M(h_c)$  is the eddy diffusivity at the canopy height, and  $\Psi_M((z_{\text{ref}} - d)/L)$  and  $\Psi_H((z_{\text{ref}} - d)/L)$  are dimensionless stability correction functions for momentum and heat, respectively (Dyer and Hicks, 1970).

The canopy ( $R_{pl}$ ) and soil ( $R_{bs}$ ) quasi-laminar boundary layer resistances depend on the trace gas  $i$  considered and were expressed following Shuttleworth and Wallace

(1985) and Choudhury and Monteith (1988), and Hicks et al. (1987), respectively, as:

$$R_{bl}^i = \frac{D_i}{D_{H_2O}} \cdot \frac{\alpha_u}{2 \cdot a \cdot LAI} \cdot \left( \frac{LW}{u(h_c)} \right)^{0.5} \cdot \left\{ 1 - \exp \left( -\frac{\alpha_u}{2} \right) \right\}^{-1} \quad (5)$$

$$R_{bs}^i = \frac{2}{k \cdot u_{*ground}} \cdot \left( \frac{Sc_i}{Pr} \right)^{2/3} \quad (6)$$

5 where  $a$  is a coefficient equal to  $0.01 \text{ s m}^{-1/2}$  (Choudhury and Monteith, 1988),  $LW$  ( $= 0.05 \text{ m}$ ) is the characteristic width of the leaves,  $D_i$  and  $D_{H_2O}$  are the diffusivities of the gas  $i$  and water vapour respectively ( $D_{O_3}/D_{H_2O} = 0.66$  and  $D_{NO_2}/D_{H_2O} = 0.62$ ; Massman, 1998),  $Sc_i$  and  $Pr$  are the Schmidt number for the gas  $i$  and the Prandtl number ( $(Sc_{O_3}/Pr)^{2/3} = 1.14$  for  $O_3$  and  $(Sc_{NO_2}/Pr)^{2/3} = 1.19$  for  $NO_2$ ; Erisman et al.,  
10 1994), and  $u_{*ground}$  is the friction velocity near the soil surface calculated following Loubet et al. (2006) as:

$$u_{*ground} = \left\{ (u^*)^2 \cdot \exp \left( 1.2 \cdot LAI \cdot \left( \frac{z_{0s}}{h_c} - 1 \right) \right) \right\}^{0.5} \quad (7)$$

where  $u_*$  is the friction velocity above the canopy.

The stomatal resistance was not modelled but used as input. It was inferred from water vapour flux measurements by inverting the Penman–Monteith equation (Monteith, 1981):  
15

$$R_{SPM}^i = \left\{ \frac{D_i}{D_{H_2O}} \cdot \frac{\frac{E}{\delta_w}}{1 + \frac{E}{\delta_w} \cdot (R_a + R_b^i) \cdot \left( \frac{\beta \cdot s}{\gamma} - 1 \right)} \right\}^{-1} \quad (8)$$

where  $E$  is the water vapour flux ( $\text{kg m}^{-2} \text{ s}^{-1}$ ),  $\delta_w$  the water vapour density saturation deficit ( $\text{kg m}^{-3}$ ),  $\beta$  the Bowen ratio,  $s$  the slope of the saturation curve ( $\text{K}^{-1}$ ) and  $\gamma$

the psychrometric constant ( $K^{-1}$ ). However,  $R_{SPM}$  can be defined as the stomatal resistance if  $E$  represents plant transpiration only, i.e. the influence of soil evaporation and evaporation of liquid water (rain, dew) that may be present at the canopy surface has to be excluded. Thus, our estimation of stomatal resistance was corrected for water evaporation as proposed by Lamaud et al. (2009): for dry conditions ( $RH < 60\%$ , for which liquid water at the leaf surface is considered to be completely evaporated)  $R_{SPM}$  was plotted against Gross Primary Production (GPP, estimated on a daily basis following Kowalski et al., 2003, 2004). The corrected stomatal resistance ( $R_s$ ) for all humidity conditions is then given by:

$$R_s^i = \frac{D_i}{D_{H_2O}} \alpha \cdot GPP^\lambda \quad (9)$$

where  $\alpha$  ( $= 7465$ ) and  $\lambda$  ( $= -1.6$ ) are coefficients given by the regression between  $R_{SPM}$  and GPP under dry conditions.

The soil and cuticular resistances to  $O_3$  deposition were expressed following Stella et al. (2011a,b) as:

$$R_{soil}^{O_3} = R_{soilmin} \cdot \exp(k_{soil} \cdot RH_{surf}) \quad (10)$$

$$R_{cut}^{O_3} = R_{cutmax} \quad \text{if } RH_{z'0} < RH_0 \quad (11a)$$

$$R_{cut}^{O_3} = R_{cutmax} \cdot \exp(-k_{cut} \cdot (RH_{z'0} - RH_0)) \quad \text{if } RH_{z'0} > RH_0 \quad (11b)$$

where  $R_{soilmin}$  ( $= 21.15 \text{ sm}^{-1}$ ) is the soil resistance without water adsorbed at the soil surface (i.e. at  $RH_{surf} = 0\%$ ),  $k_{soil}$  ( $= 0.024$ ) is an empirical coefficient of the exponential function,  $R_{cutmax}$  ( $= 5000/LAI$ ) is the maximal cuticular resistance calculated according to Massman (2004),  $RH_0$  ( $= 60\%$ ) is a threshold value of the relative humidity,  $k_{cut}$  ( $= 0.045$ ) is an empirical coefficient of the exponential function taken from Lamaud et al. (2009), and  $RH_{surf}$  and  $RH_{z'0}$  are the relative humidity at the soil and leaf surface, respectively, calculated by the energy balance model.

## Measurements of nitrogen oxides and ozone fluxes

P. Stella et al.

Title Page

Abstract

Introduction

Conclusions

References

Tables

Figures

◀

▶

◀

▶

Back

Close

Full Screen / Esc

Printer-friendly Version

Interactive Discussion



## Measurements of nitrogen oxides and ozone fluxes

P. Stella et al.

Title Page

Abstract

Introduction

Conclusions

References

Tables

Figures

◀

▶

◀

▶

Back

Close

Full Screen / Esc

Printer-friendly Version

Interactive Discussion



Concerning the NO<sub>2</sub> cuticular resistance, several studies showed that this deposition pathway did not contribute significantly to NO<sub>2</sub> deposition and could be neglected (Rondón et al., 1993; Segschneider et al., 1995; Gut et al., 2002). Consequently,  $R_{\text{cut}}^{\text{NO}_2}$  was set to 9999 s m<sup>-1</sup>. Since an empirical parameterization for the soil resistance to NO<sub>2</sub> deposition is currently not available, a constant value ( $R_{\text{soil}}^{\text{NO}_2} = 340 \text{ s m}^{-1}$ ) reported by Gut et al. (2002) for a soil in the Amazonian rain forest was used.

Finally, many trace gases entering into plants through stomata can react with compounds in the sub-stomatal cavity and the mesophyll. For O<sub>3</sub>, there is evidence that  $R_{\text{int}}$  is usually zero (Erismann et al., 1994). However, for NO<sub>2</sub> there is currently no consensus concerning the existence of an internal resistance, and the uncertainty of the magnitude of its contribution to the overall surface resistance is large. Due to this insufficient knowledge,  $R_{\text{int}}$  was also set to zero for NO<sub>2</sub> in the “a priori” model parameterization.

The total deposition flux of the scalar  $i$  ( $F_i$ ) is the sum of deposition flux to the soil ( $F_{\text{soil}}^i$ ) and the deposition flux to the vegetation ( $F_{\text{veg}}^i$ ):

$$F_i = F_{\text{soil}}^i + F_{\text{veg}}^i \quad (12)$$

In analogy to Ohm’s law and following the resistive scheme of the Surf atm model (Fig. 1), total, vegetation and soil fluxes can be expressed as:

$$F_i = \frac{\chi_i(z_0) - \chi_i(z_{\text{ref}})}{R_a(z_{\text{ref}})} \quad (13)$$

$$F_{\text{veg}}^i = \frac{-\chi_i(z_0)}{R_{\text{bl}}^i + \left[ \frac{1}{R_{\text{cut}}^i} + \frac{1}{R_s^i + R_{\text{int}}^i} \right]^{-1}} \quad (14)$$

$$F_{\text{soil}}^i = \frac{-\chi_i(z_0)}{R_{\text{ac}} + R_{\text{bs}}^i + R_{\text{soil}}^i} \quad (15)$$

The deposition flux to soil can also be expressed as:

$$F_{\text{soil}}^i = \frac{\chi_i(z_{0s}) - \chi_i(z_0)}{R_{\text{ac}}} \quad (16)$$

$$F_{\text{soil}}^i = \frac{-\chi_i(z_{0s})}{R_{\text{bs}}^i + R_{\text{soil}}^i} \quad (17)$$

## 5 2.6 Chemical reaction and transport times

In contrast to inert gases such as CO<sub>2</sub> and H<sub>2</sub>O, the fluxes of NO, NO<sub>2</sub> and O<sub>3</sub> could be subject to chemical reactions leading to non-constant fluxes with height (vertical flux divergence). According to Remde et al. (1993) and Warneck (2000), the main gas phase reactions for the NO-O<sub>3</sub>-NO<sub>2</sub> triad are:



where  $k_r$  is the rate constant of R1 (Atkinson et al., 2004) and  $j_{\text{NO}_2}$  is the photolysis frequency for R2.

15 The chemical reaction time for NO-O<sub>3</sub>-NO<sub>2</sub> triad ( $\tau_{\text{chem}}$  in s) gives the characteristic time scale of the set of R1 and R2. It was estimated following the approach of Lenschow (1982):

$$\tau_{\text{chem}} = 2 \left/ \left[ j_{\text{NO}_2}^2 + k_r^2 \cdot (\text{O}_3 - \text{NO})^2 + 2 \cdot j_{\text{NO}_2} \cdot k_r (\text{O}_3 + \text{NO} + 2 \cdot \text{NO}_2) \right]^{0.5} \right. \quad (18)$$

In addition, the characteristic chemical depletion times for NO, O<sub>3</sub> and NO<sub>2</sub> were calculated according to De Arellano and Duynderke (1992):

$$\tau_{\text{deplNO}} = \frac{1}{k_r \cdot \text{O}_3} \quad (19a)$$

$$\tau_{\text{deplO}_3} = \frac{1}{k_r \cdot \text{NO}} \quad (19b)$$

$$5 \quad \tau_{\text{deplNO}_2} = \frac{1}{j_{\text{NO}_2}} \quad (19c)$$

The comparison of characteristic chemical reaction times with characteristic turbulent transport times indicates whether or not there is a significant vertical divergence of the turbulent flux of reactive trace gases. The transport time ( $\tau_{\text{trans}}$  in s) in one layer (i.e. above the canopy, between the measurement height and the canopy top, or within the canopy) can be expressed as the aerodynamic resistance through each layer multiplied by the layer thickness (Garland, 1977):

$$\tau_{\text{trans}} = R_a(z_{\text{ref}}) \cdot (z_{\text{ref}} - d - z_0) \quad \text{above the canopy} \quad (20a)$$

$$15 \quad \tau_{\text{trans}} = R_{\text{ac}} \cdot (d + z_0 - z_{0s}) \quad \text{within the canopy} \quad (20b)$$

The ratio between  $\tau_{\text{trans}}$  and  $\tau_{\text{chem}}$  is defined as the Damköhler number (DA) (Damköhler, 1940):

$$DA = \frac{\tau_{\text{trans}}}{\tau_{\text{chem}}} \quad (21)$$

According to Damköhler (1940), the divergence of a reactive trace gas flux is negligible if  $DA \ll 1$  (conventionally  $DA \leq 0.1$ ), i.e. the turbulent transport is much faster than chemical reactions and consequently, the reactive trace gas can be considered as a (quasi-)passive tracer. For  $DA > 0.1$  measured reactive trace gas fluxes have to be corrected for the influence of (fast) chemical reactions to obtain correct turbulent fluxes of the reactive trace gas.



humidity (RH) decreased during the morning to reach its minimum of 65 % after noon (Fig. 2b). The meteorological conditions were different during the first half of the experiment (29 August to 9 September 2005) and the second half (10 to 20 September 2005). While the former period was sunny and warm and characterized by easterly flows, the latter was dominated by rainy, cold, and overcast conditions governed by westerly winds. This resulted in considerable variability of the meteorological conditions during the experiment: maximal  $G_r$  and  $T_a$  ranged between 200–800  $Wm^{-2}$ , and 15–25 °C, respectively, and minimal RH varied between 80–50 % (Fig. 2a, b).

Mean diel courses of  $NO_2$ , NO and  $O_3$  mixing ratios measured at 1.65 m a.g.l. (profile system) are shown in Fig. 2c. Median NO mixing ratios were close to zero during the major part of the experiment and slightly increased during the morning to about 1 ppb. These elevated NO values occurred when the  $NO_2$  mixing ratio began to decrease due to photolysis. In addition, some NO was most likely advected from roads passing the site at a distance of 2 km in NE from the experimental site. Highest mixing ratios of  $NO_2$  were on average about 6 ppb during the early morning and 4 ppb during the late afternoon, but increased occasionally up to 8 ppb. During the rest of the day,  $NO_2$  mixing ratios were around 2–3 ppb. The diel trend of  $NO_2$  was linked with photochemistry: during sunrise,  $NO_2$  photolysis led to the decrease in  $NO_2$  mixing ratios, while during nighttime the absence of photolysis and the stable stratification induced an accumulation of  $NO_2$  in the lower troposphere.  $O_3$  mixing ratios exceeded NO and  $NO_2$  mixing ratios and varied from 10 to 20 ppb during nighttime and from 40 to 60 ppb during daytime. During the morning, turbulent mixing in the planetary boundary layer led to entrainment of  $O_3$  from the free troposphere (Stull, 1989). In addition, photochemical  $O_3$  production (in the presence of  $NO_x$  and volatile organic compounds) caused the increase of  $O_3$  mixing ratios during the morning, reaching its maximum in the early afternoon. The  $O_3$  removal by dry deposition processes and the reduced entrainment of  $O_3$  from the free troposphere as a result of thermally stable stratification and low wind conditions induced a decrease in  $O_3$  mixing ratio during late afternoon and particularly

## BGD

10, 4461–4514, 2013

### Measurements of nitrogen oxides and ozone fluxes

P. Stella et al.

Title Page

Abstract

Introduction

Conclusions

References

Tables

Figures

⏪

⏩

◀

▶

Back

Close

Full Screen / Esc

Printer-friendly Version

Interactive Discussion



during the night (c.f., Coyle et al., 2002). Overall, NO<sub>2</sub> and O<sub>3</sub> mixing ratios were higher from 29 August 2005 to 9 September 2005 than from 10 to 20 September 2005.

### 3.2 Footprint analysis and measured fluxes

Since the three-pod mast, the laboratory container and some rural settlements were potentially distorting the flow in the north and in the eastern sector of our site, we performed a footprint analysis according to Göckede et al. (2004, 2006). Owing to the extended fetch in western, southern and south-eastern directions, the major part of the fluxes measured by the EC systems originated from the experimental field, independently of the stability conditions (Fig. 3). However, the surrounding areas contributed to the total fluxes mainly in the NNW/NE sectors, due to (i) the limited fetch and (ii) the rural settlements disturbing the flow in these directions. In addition, the footprint area increased with atmospheric stability. In order to ensure that only those measured fluxes which originated from the experimental field (and not from the surrounding areas) were used for subsequent analyses, we considered only those 30 min flux data for which at least 95 % of the total footprint area could be attributed to the experimental field.

NO<sub>2</sub> and O<sub>3</sub> fluxes were directed downward, i.e. net deposition fluxes were observed (Fig. 2d). Both NO<sub>2</sub> and O<sub>3</sub> deposition fluxes were close to zero during night-time and typically increased during the morning to their maximum. Maximum deposition fluxes of NO<sub>2</sub> occurred in the early morning and ranged on average from about  $-0.3 \text{ nmol m}^{-2} \text{ s}^{-1}$  to  $-0.6 \text{ nmol m}^{-2} \text{ s}^{-1}$ . The deposition fluxes of O<sub>3</sub> were about 10 to 20 times higher than NO<sub>2</sub> fluxes ranging on average from  $-7 \text{ nmol m}^{-2} \text{ s}^{-1}$  to  $-12 \text{ nmol m}^{-2} \text{ s}^{-1}$  at noon. The calculated deposition velocities for NO<sub>2</sub> and O<sub>3</sub> exhibited a similar diel course and increased during the morning, reaching their maximum and decreasing during afternoon. Despite similar deposition velocities during night-time ( $\sim 0.1 \text{ cm s}^{-1}$ ), the maximal median deposition velocity for NO<sub>2</sub> was two times lower than for O<sub>3</sub> during daytime (around  $0.3 \text{ cm s}^{-1}$  for NO<sub>2</sub> and  $0.6 \text{ cm s}^{-1}$  for O<sub>3</sub>) (Fig. 2e). NO fluxes measured by EC during the field experiment were close to zero

BGD

10, 4461–4514, 2013

## Measurements of nitrogen oxides and ozone fluxes

P. Stella et al.

Title Page

Abstract

Introduction

Conclusions

References

Tables

Figures

◀

▶

◀

▶

Back

Close

Full Screen / Esc

Printer-friendly Version

Interactive Discussion



during nighttime and were directed upward during daytime, i.e. indicating net emission, with maxima of 0.05–0.1 nmol m<sup>-2</sup> s<sup>-1</sup> during daytime (see Fig. 2d).

### 3.3 Model vs. measurements: fluxes and mixing ratios

The O<sub>3</sub> fluxes estimated using the Surf atm model agreed well with those measured during the whole experimental period. The linear regression showed that the model underestimated the measured fluxes by only 2% on average (Fig. 4a). We attempted another step of validation of the Surf atm model by comparing measured and model derived O<sub>3</sub> mixing ratios at two crucial levels, namely at  $z_0$  and  $z_{0s}$ . For that O<sub>3</sub> mixing ratios were estimated (a) at  $z_0$  estimated from Eq. (13) using the measured O<sub>3</sub> flux, the measured O<sub>3</sub> mixing ratio at  $z_{ref}$  and modelled  $R_a$ , and (b) at  $z_{0s}$  from Eq. (16) using the modelled O<sub>3</sub> soil flux, the measured O<sub>3</sub> mixing ratio at 20 cm (later moved at 28 cm) and modelled  $R_{ac}$  values. In Fig. 4b, c these O<sub>3</sub> mixing ratios are shown in comparison (a) to the O<sub>3</sub> mixing ratio measured at 20–28 cm assuming that 20–28 cm was representative of  $z_0$ , and (b) to the measured O<sub>3</sub> mixing ratio at 5 cm assuming that this level was representative of  $z_{0s}$ . At least during daytime, the modelled O<sub>3</sub> mixing ratios just above the canopy and the soil agree very well with the measurement, which validates the applied values of  $R_a$  and  $R_{ac}$  (necessary to estimate transport times above and within the canopy; see Sect. 2.6). This result is indeed justified also by the fact, that O<sub>3</sub> mixing ratios modelled with  $\pm 50\%$  of  $R_a$  and  $R_{ac}$  (red dashed lines in Figs. 4b, c) largely deviate from measured mixing ratios. The good agreement for O<sub>3</sub> indicates that the resistances used to model O<sub>3</sub> fluxes were valid and consequently represent the O<sub>3</sub> exchange processes quite well.

The turbulent resistances (i.e.  $R_a$  and  $R_{ac}$ ) used to model NO<sub>2</sub> deposition fluxes are identical to those used for modelling the O<sub>3</sub> fluxes (only modulated by different molecular diffusivities; see Sect. 2.5). Thus, the good agreement between measured and modelled O<sub>3</sub> fluxes and mixing ratios would suggest to apply resistances  $R_a$ ,  $R_{ac}$ ,  $R_{bl}$ ,  $R_{bs}$ , and  $R_s$  also for the simulation of NO<sub>2</sub> deposition fluxes.

BGD

10, 4461–4514, 2013

## Measurements of nitrogen oxides and ozone fluxes

P. Stella et al.

Title Page

Abstract

Introduction

Conclusions

References

Tables

Figures

◀

▶

◀

▶

Back

Close

Full Screen / Esc

Printer-friendly Version

Interactive Discussion



**Measurements of  
nitrogen oxides and  
ozone fluxes**

P. Stella et al.

[Title Page](#)[Abstract](#)[Introduction](#)[Conclusions](#)[References](#)[Tables](#)[Figures](#)[◀](#)[▶](#)[◀](#)[▶](#)[Back](#)[Close](#)[Full Screen / Esc](#)[Printer-friendly Version](#)[Interactive Discussion](#)

However, a priori modelled  $\text{NO}_2$  deposition fluxes (with  $R_{\text{int}}^{\text{NO}_2} = 0$ ) do not agree well with the measured  $\text{NO}_2$  fluxes during the SALSA campaign (Fig. 5). The relationship between measured and modelled  $\text{NO}_2$  fluxes showed a significant scatter ( $R^2 = 0.45$ ) and a large deviation (slope = 1.22) from the 1 : 1 line (Fig. 5a). The  $\text{NO}_2$  fluxes during nighttime were quite well reproduced by the model with an absolute difference varying around zero (Fig. 5b). However, this small absolute difference caused a large relative difference between measured and modelled fluxes, indicating an underestimation by the model of around 50 %, which was due to the small  $\text{NO}_2$  fluxes during nighttime (Fig. 2d). Nevertheless, during daytime the  $\text{NO}_2$  deposition was significantly overestimated. The difference between measured and modelled  $\text{NO}_2$  fluxes increased during the morning, reached its maximum at noon and decreased during the afternoon (Fig. 5b). At noon, the modelled  $\text{NO}_2$  fluxes were typically two times larger than the measured  $\text{NO}_2$  fluxes, and this overestimation could occasionally reach a factor of three (Fig. 5b).

It is now required to understand the reasons responsible for this substantial overestimation of the a priori modelled  $\text{NO}_2$  deposition. These reasons could be separated in two categories: (i) the measured  $\text{NO}_2$  fluxes were not only caused by turbulent transport of  $\text{NO}_2$  towards the surface and/or (ii) the resistances to  $\text{NO}_2$  deposition used in the model were underestimated. On one hand, the EC method measures the flux at a specific height ( $z_{\text{ref}} = 2$  m). For reactive species such as  $\text{NO}_2$ , chemical reactions in the air column within or above the canopy could induce a flux divergence with height, meaning that the flux at the measurement height is different than the flux close to the surface, which is in contrast to inert species such as water vapour or  $\text{CO}_2$  (e.g. Kramm et al., 1991, 1996; Galmarini et al., 1997; Walton et al., 1997). If the characteristic turbulent transport times (see Eq. 20) are not significantly shorter than characteristic chemical reaction times (see Eq. 18), these processes could also induce lower deposition fluxes measured at a height of 2 m. In addition, the EC flux measurements represent the net exchange resulting from the balance between emission and deposition processes. In case the  $\text{NO}_2$  fluxes would be bi-directional, which would imply that a surface source for

NO<sub>2</sub> exists, the deposition flux estimated by the model would be larger than the measured net flux. On the other hand, the model could also overestimate NO<sub>2</sub> deposition, which implies that the applied resistance parameterisations in the model might be not complete. However, as explained previously, this was not the case for  $R_a$ ,  $R_{ac}$ ,  $R_{bl}$ ,  $R_{bs}$ , and  $R_s$  since they were validated owing to the good agreement between measured and modelled O<sub>3</sub> fluxes. Thus, if we presume that the cuticular deposition is negligible (i.e.  $R_{cut}^{NO_2} = 9999 \text{ s m}^{-1}$ ) as shown previously (see above), only the remaining resistances  $R_{soil}$  and  $R_{int}$  for NO<sub>2</sub> could be underestimated. In the following, each reason that may explain the overestimation of NO<sub>2</sub> deposition by the model is explored and discussed.

### 3.4 Impact of chemical reactions on NO<sub>2</sub> fluxes

Transport and chemical reaction times were estimated above and within the canopy in order to determine to what extent chemical depletion or production in the air column could affect the measured NO<sub>2</sub> fluxes.

Characteristic transport times ( $\tau_{trans}$ ) for both above and within the canopy followed a diurnal cycle (Fig. 6a). It was larger during nighttime and decreased during the morning to reach its minimum in the early afternoon. It then increased during the afternoon until the sunset. Despite the difference of the layer height (above the canopy:  $z_{ref} - d = 1.60 \text{ m}$  and  $1.50 \text{ m}$  at the beginning and the end of the experiment, respectively; within the canopy:  $d - z_{0s} = 0.10 \text{ m}$  and  $0.19 \text{ m}$  at the beginning and the end of the experiment, respectively),  $\tau_{trans}$  was comparable above the canopy and within the canopy. It was about 200 s during nighttime and decreased to about 55 s above the canopy and to 80 s within the canopy at noon. The lower turbulence and stable atmospheric conditions during nighttime induced a slower turbulent transport, while the unstable atmospheric conditions and turbulent mixing enhanced reduced  $\tau_{trans}$ . Although  $\tau_{trans}$  was comparable above and within the canopy, it must be kept in mind that the layer height was different, being 1.50 m above and only 0.20 m within the canopy.

BGD

10, 4461–4514, 2013

## Measurements of nitrogen oxides and ozone fluxes

P. Stella et al.

Title Page

Abstract

Introduction

Conclusions

References

Tables

Figures

◀

▶

◀

▶

Back

Close

Full Screen / Esc

Printer-friendly Version

Interactive Discussion



This implies that the “transfer velocity” was significantly lower within the canopy than above.

Characteristic chemical reaction times were calculated above and within the canopy. Above the canopy,  $\tau_{\text{chem}}$  was calculated using Eq. (18), i.e. taking into account both  $\text{NO}_2$  photolysis and  $\text{NO}_2$  production by the reaction between  $\text{O}_3$  and  $\text{NO}$ . However,  $j_{\text{NO}_2}$  was not measured inside the canopy, hence;  $\tau_{\text{chem}}$  could not be calculated using Eq. (18). Since  $j_{\text{NO}_2}$  is closely related to  $G_r$  (see Trebs et al., 2009), which typically sharply decreases in a dense canopy,  $\text{NO}_2$  photolysis was assumed to be negligible. In addition, the measured  $\text{O}_3$  mixing ratio at 0.05 m above ground level was about 10 times larger than the measured  $\text{NO}$  mixing ratio in the early morning and up to 30 times larger during the afternoon and nighttime (data not shown). The reaction between  $\text{NO}$  and  $\text{O}_3$  is a second order reaction, but can be approximated by a pseudo-first order reaction because  $\text{O}_3$  was in excess compared to  $\text{NO}$ . The pseudo-first order reaction rate constant is defined as  $k'_r = k_r \cdot \text{O}_3$  (in  $\text{s}^{-1}$ ), and  $\tau_{\text{chem}}$  inside the canopy can be approximated as the chemical depletion time for  $\text{NO}$  (Eq. 19a). The chemical reaction time followed the same diurnal cycle above and within the canopy: it reached its maximum in the early morning, progressively decreased to reach a minimum in early afternoon, and increased from the early afternoon to the early morning (Fig. 6b). Despite of the comparable diurnal cycle above and within the canopy  $\tau_{\text{chem}}$  above the canopy was usually faster than inside the canopy. The chemical reaction time above the canopy peaked at 300 s and decreased to 80 s, whereas inside the canopy it reached 600 s and decreased to only 150 s (Fig. 6b).

The DA values calculated from Eq. (21) were usually lower than unity, implying that in general turbulent transport was faster than chemical reactions, although DA was occasionally close to unity (Fig. 6c). In addition, DA was larger above the canopy than within the canopy due to the faster chemical reaction time above the canopy. DA values varied between 0.3 and 0.7 within the canopy and ranged from 0.5 to unity above the canopy. Damköhler (1940) stated that a trace gas can be treated as a non-reactive tracer for  $\text{DA} \ll 1$ . However, it is now generally accepted by the scientific community that a gas

## Measurements of nitrogen oxides and ozone fluxes

P. Stella et al.

[Title Page](#)[Abstract](#)[Introduction](#)[Conclusions](#)[References](#)[Tables](#)[Figures](#)[⏪](#)[⏩](#)[◀](#)[▶](#)[Back](#)[Close](#)[Full Screen / Esc](#)[Printer-friendly Version](#)[Interactive Discussion](#)

can be treated as non-reactive only for  $DA < 0.1$ , and that chemical divergence could be of minor importance for  $0.1 < DA < 1$ . For example, Stella et al. (2012) demonstrated that chemical reactions induced a flux divergence for  $O_3$  and  $NO$  accounting for 0 % to 25 % of the measured fluxes for  $0.1 < DA < 1$ .

Consequently, the impact of chemistry above the canopy on measured  $NO_2$  fluxes was evaluated using the method proposed by Duyzer et al. (1995). According to this method, chemistry between  $NO$ ,  $NO_2$  and  $O_3$  above the canopy could induce only a small divergence. The median difference between the measured and the corrected  $NO_2$  fluxes varied between  $\pm 0.025 \text{ nmol m}^{-2} \text{ s}^{-1}$ , which corresponded to a relative difference of  $\pm 10 \%$  (Fig. 7a), whereas the difference between measured and modelled  $NO_2$  fluxes was about 20 times larger (absolute difference  $\approx 0.40 \text{ nmol m}^{-2} \text{ s}^{-1}$ , ratio  $\approx 2$  during daytime; see Fig. 5b and Sect. 3.3). Hence, chemistry above the canopy did not explain the large overestimation of  $NO_2$  deposition fluxes by the model. In addition, similarly to  $O_3$ , the  $NO_2$  mixing ratio was estimated at  $z_0$  from Eq. (13) using the measured  $NO_2$  flux, the measured  $NO_2$  mixing ratio at  $z_{\text{ref}}$  and modelled  $R_a$ , and compared with  $NO_2$  mixing ratio estimated at 20–28 cm (Fig. 7b). Since the resistance analogy implies the absence of chemical reactions, the good agreement between measured and modelled  $NO_2$  mixing ratio above the canopy also confirmed the non significance of chemistry above the canopy, at least during daytime. Nevertheless, during nighttime, discrepancies occurred between measured and modelled  $NO_2$  mixing ratios, meaning that fast chemistry cannot be discarded.

These methods could not be used to estimate the influence of chemical reactions inside the canopy since (i) the method proposed by Duyzer et al. (1995) is only based on mass conservation of the  $NO$ - $O_3$ - $NO_2$  triad and it does not integrate the different emission or deposition processes that could occur inside the canopy, and (ii) the comparison of measured and modelled  $NO_2$  mixing ratios inside the canopy (i.e. at 5 cm) requires knowledge of the modelled soil  $NO_2$  flux, or at least the vegetation flux (to deduce the soil flux from the difference between total and vegetation  $NO_2$  flux), which cannot be estimated without knowledge of the  $NO_2$  internal resistance. However, our

**BGD**

10, 4461–4514, 2013

## Measurements of nitrogen oxides and ozone fluxes

P. Stella et al.

Title Page

Abstract

Introduction

Conclusions

References

Tables

Figures

◀

▶

◀

▶

Back

Close

Full Screen / Esc

Printer-friendly Version

Interactive Discussion



results suggest that the impact of NO-O<sub>3</sub>-NO<sub>2</sub> chemistry inside the canopy could be negligible. The calculated DA numbers did not indicate that chemistry was dominating the exchange inside the canopy. In addition, the DA number inside the canopy was lower than above the canopy (Fig. 6c), which implies that chemistry inside the canopy was probably even less important than above the canopy.

### 3.5 Compensation point for NO<sub>2</sub>

In order to investigate the existence of a NO<sub>2</sub> emission flux that may partially compensate the NO<sub>2</sub> deposition flux, thus, causing an overestimation of the modelled NO<sub>2</sub> deposition flux, the existence of a canopy compensation point (the NO<sub>2</sub> mixing ratio just above the vegetation elements at which consumption and production processes balance each other) was explored. Figure 8 shows the measured NO<sub>2</sub> fluxes corrected for chemical reactions above the canopy versus the measured NO<sub>2</sub> mixing ratios. Only data for  $G_r > 400 \text{ Wm}^{-2}$  were considered, a threshold above which stomatal conductance is supposed to be constant. The linear regression between the NO<sub>2</sub> flux and the NO<sub>2</sub> mixing ratio did not show an intersection of the regression line with the x-axis (NO<sub>2</sub> mixing ratio) within the error of the regression at the 95 % confidence interval. Hence, these results do not suggest the existence of a canopy compensation point, and thus indicate the non-existence of a NO<sub>2</sub> emission flux at the meadow. In addition, this result also supports the small influence of chemical NO<sub>2</sub> production inside the canopy, as stated previously.

The existence of the NO<sub>2</sub> compensation point, as well as its magnitude, is currently subject to debate (Lerdau et al., 2000). Numerous studies carried out over several ecosystems such as forests, crops and grasslands reported NO<sub>2</sub> compensation points on the leaf or branch level ranging from less than 0.1 ppb to up to 1.5 ppb (Johansson, 1987; Weber and Rennenberg, 1996; Gebler et al., 2000, 2002; Hereid and Monson, 2001; Teklemariam and Sparks, 2006). However, these studies used (i) non-specific NO<sub>2</sub> detection techniques using molybdenum or iron sulphate converters and (ii) chamber methods to measure the exchange of NO<sub>2</sub> at the leaf level. These methods

## Measurements of nitrogen oxides and ozone fluxes

P. Stella et al.

Title Page

Abstract

Introduction

Conclusions

References

Tables

Figures

◀

▶

◀

▶

Back

Close

Full Screen / Esc

Printer-friendly Version

Interactive Discussion



could lead to an overestimation of the NO<sub>2</sub> compensation point estimation due to (i) overestimation of the NO<sub>2</sub> mixing ratio (Parrish and Fehsenfeld, 2000; Dunlea et al., 2007; Dari-Salisburgo et al., 2009) and (ii) underestimation of the NO<sub>2</sub> deposition flux due to chemistry inside the chambers as discussed by Meixner et al. (1997), Pape et al. (2009), Chaparro-Suarez (2011) and Breuninger et al. (2012). Our results underline the findings of Gut et al. (2002) on Amazonian forest trees and by Segschneider et al. (1995) on sunflower. In addition, Chaparro-Suarez et al. (2011) and Breuninger et al. (2012), who made measurements on pine, birch, beech and oak using a specific NO<sub>2</sub> converter (see Sect. 2.3) and performed corrections for chemical reactions inside the chamber, did not find a compensation point for NO<sub>2</sub>.

### 3.6 Model sensitivity to soil resistance for NO<sub>2</sub>

A sensitivity analysis of the Surf atm model to  $R_{\text{soil}}^{\text{NO}_2}$  was made in order to evaluate to what extent a potential underestimation of the NO<sub>2</sub> soil resistance could explain the overestimation of the a priori modelled NO<sub>2</sub> deposition fluxes. The NO<sub>2</sub> deposition flux was modelled using four different soil resistances ( $R_{\text{soil}}^{\text{NO}_2} = 500 \text{ sm}^{-1}$ ,  $R_{\text{soil}}^{\text{NO}_2} = 1000 \text{ sm}^{-1}$ ,  $R_{\text{soil}}^{\text{NO}_2} = 2000 \text{ sm}^{-1}$ , and  $R_{\text{soil}}^{\text{NO}_2} = 9999 \text{ sm}^{-1}$ ) and compared to the reference case (i.e.  $R_{\text{soil}}^{\text{NO}_2} = 340 \text{ sm}^{-1}$ ).

The modelled NO<sub>2</sub> deposition decreased when  $R_{\text{soil}}^{\text{NO}_2}$  increased (Fig. 9). However, the sensitivity of the model result to  $R_{\text{soil}}^{\text{NO}_2}$  was dependent on the time of the day. The relative decrease of the modelled NO<sub>2</sub> deposition flux with increasing  $R_{\text{soil}}^{\text{NO}_2}$  was less marked during daytime than during nighttime. It was around 1.5 %, 4 %, 8.5 %, and 16 % during daytime for  $R_{\text{soil}}^{\text{NO}_2}$  equal to 500 sm<sup>-1</sup>, 1000 sm<sup>-1</sup>, 2000 sm<sup>-1</sup>, and 9999 sm<sup>-1</sup>, respectively, whereas during nighttime the increase of  $R_{\text{soil}}^{\text{NO}_2}$  caused a decrease of the modelled NO<sub>2</sub> deposition flux of around 4 %, 13 %, 25 %, and 240 % for the four cases considered (Fig. 9).

BGD

10, 4461–4514, 2013

## Measurements of nitrogen oxides and ozone fluxes

P. Stella et al.

Title Page

Abstract

Introduction

Conclusions

References

Tables

Figures

◀

▶

◀

▶

Back

Close

Full Screen / Esc

Printer-friendly Version

Interactive Discussion



## Measurements of nitrogen oxides and ozone fluxes

P. Stella et al.

Title Page

Abstract

Introduction

Conclusions

References

Tables

Figures

◀

▶

◀

▶

Back

Close

Full Screen / Esc

Printer-friendly Version

Interactive Discussion



This diurnal variation was due to the change of the  $\text{NO}_2$  deposition pathways during the course of the day. During daytime,  $\text{NO}_2$  is deposited through stomatal and soil pathways, the former representing the main  $\text{NO}_2$  removal pathway (Rondón et al., 1993; Gut et al., 2002). Since  $\text{NO}_2$  soil deposition represents only a small part of the total depo-  
 5 sition, any increase of  $R_{\text{soil}}^{\text{NO}_2}$  does not induce a large modification of the modelled  $\text{NO}_2$  deposition flux. Conversely, the soil pathway represents the only sink for  $\text{NO}_2$  during nighttime. Thus, the sensitivity of the modelled  $\text{NO}_2$  flux to  $R_{\text{soil}}^{\text{NO}_2}$  is larger.

Obviously, a potential underestimation of  $R_{\text{soil}}^{\text{NO}_2}$  did not explain the observed discrepancy between measured and modelled  $\text{NO}_2$  fluxes. For realistic values of  $R_{\text{soil}}^{\text{NO}_2}$   
 10 ( $500 \text{ s m}^{-1}$  and  $1000 \text{ s m}^{-1}$ ) the modelled  $\text{NO}_2$  fluxes were only less than 5 % lower during daytime than the fluxes modelled with  $R_{\text{soil}}^{\text{NO}_2} = 340 \text{ s m}^{-1}$ , whereas the model overestimated measurements by about a factor of two (Fig. 5b). Even if we assume that the soil deposition was zero (i.e.  $R_{\text{soil}}^{\text{NO}_2} = 9999 \text{ s m}^{-1}$ ), that would only led to a model overestimation of 13 %.

Consequently, neither the underestimation of  $R_{\text{soil}}^{\text{NO}_2}$  nor chemical divergence within  
 15 and above the canopy or  $\text{NO}_2$  emission from vegetation explained the large overestimation of the  $\text{NO}_2$  deposition fluxes by the model during daytime. In addition,  $R_a$ ,  $R_{ac}$ ,  $R_{bl}$ ,  $R_{bs}$ , and  $R_s$  were already validated owing to the good agreement between measured and modelled  $\text{O}_3$  fluxes (see Sect. 3.3). These facts prove that the only process that  
 20 could explain the overestimation of the modelled  $\text{NO}_2$  deposition flux is the existence of an internal resistance for  $\text{NO}_2$ , which was ignored in the modelling approach.

### 3.7 Internal resistance for $\text{NO}_2$

In the a priori model parameterisation presented above the internal resistance for  $\text{NO}_2$   
 25 was set to zero. According to the pervious results, only the existence of a significant internal resistance could explain the large discrepancy between measured and modelled  $\text{NO}_2$  fluxes. In order to estimate the magnitude of  $R_{\text{int}}^{\text{NO}_2}$ ,  $\text{NO}_2$  fluxes were modelled

## Measurements of nitrogen oxides and ozone fluxes

P. Stella et al.

Title Page

Abstract

Introduction

Conclusions

References

Tables

Figures

◀

▶

◀

▶

Back

Close

Full Screen / Esc

Printer-friendly Version

Interactive Discussion

including several values of  $R_{\text{int}}^{\text{NO}_2}$  (i.e.  $50 \text{ s m}^{-1}$  to  $500 \text{ s m}^{-1}$ , with steps of  $50 \text{ s m}^{-1}$ ). The results are summarized in Table 2. Following this analysis, it is not clear what was the best value for  $R_{\text{int}}^{\text{NO}_2}$ . The best slope of the regression (0.94) was found for  $R_{\text{int}}^{\text{NO}_2} = 100 \text{ s m}^{-1}$ , but the lowest RMSE ( $0.21 \text{ nmol m}^{-2} \text{ s}^{-1}$ ) was found for a value of  $R_{\text{int}}^{\text{NO}_2} = 150 \text{ s m}^{-1}$ . Hence, we also deduced  $R_{\text{int}}^{\text{NO}_2}$  in an alternative empirical approach from the  $\text{NO}_2$  flux measurements by inverting the resistive scheme (leaving all other resistances as described above for the a priori approach). For large  $R_{\text{s}}^{\text{NO}_2}$  values that have a high relative uncertainty, this calculation procedure may lead to errors and sometimes even to negative values of  $R_{\text{int}}^{\text{NO}_2}$ . Hence, only data for  $1/R_{\text{s}}^{\text{NO}_2} > 0.2 \text{ cm s}^{-1}$  ( $R_{\text{s}}^{\text{NO}_2} < 500 \text{ s m}^{-1}$ ) were considered.

The magnitude of  $R_{\text{int}}^{\text{NO}_2}$  was highly variable throughout the day (Fig. 10a). It was close to zero during the early morning and progressively increased to  $200 \text{ s m}^{-1}$  at noon. The maximal median of  $R_{\text{int}}^{\text{NO}_2}$  was prevailing during the early afternoon and was about  $300 \text{ s m}^{-1}$ . The averaged  $R_{\text{int}}^{\text{NO}_2}$  was  $165 \text{ s m}^{-1}$ , but the magnitude of the estimated  $R_{\text{int}}^{\text{NO}_2}$  varied considerably and ranged from  $100 \text{ s m}^{-1}$  to  $800 \text{ s m}^{-1}$  (interquartile range). In comparison,  $R_{\text{s}}^{\text{NO}_2}$  was around  $400 \text{ s m}^{-1}$  during the early morning and progressively decreased to  $100 \text{ s m}^{-1}$ . It then increased again during the early afternoon (Fig. 10a). The contribution of  $R_{\text{int}}^{\text{NO}_2}$  to the total leaf resistance varied during the day. The contribution was close to zero during the early morning but increased to represent between 50 % and 90 % (interquartile range), with the median contribution of  $R_{\text{int}}^{\text{NO}_2}$  to the total leaf resistance estimated to 75 % during the early afternoon (Fig. 10b).

In contrary to the results obtained by Segschneider et al. (1995) for sunflower and Geßler et al. (2000, 2002) for beech and spruce, we found the existence of a leaf internal resistance for  $\text{NO}_2$ . The results obtained during this study confirmed those obtained by Jonhansson (1987) and Gut et al. (2002), who reported significant values

of  $R_{\text{int}}^{\text{NO}_2}$  ranging from  $10 \text{ s m}^{-1}$  to  $2000 \text{ s m}^{-1}$ . As reported in these previous studies  $R_{\text{int}}^{\text{NO}_2}$  contributed significantly to the total leaf resistance. Nevertheless, its contribution was slightly larger than reported by Jonhansson (1987) who indicated that  $R_{\text{int}}^{\text{NO}_2}$  represented between 3 % and 60 % to the total leaf resistance, and by Gut et al. (2002) and  
5 Chaparro-Suarez (2011), who both estimated that  $R_{\text{int}}^{\text{NO}_2}$  accounted for 40 % of the total leaf resistance.

Both  $R_{\text{int}}^{\text{NO}_2}$  and its contribution to the total leaf resistance exhibited a diurnal cycle: they increased during the morning but did not decrease in the same proportion during the afternoon. The underlying processes responsible for  $R_{\text{int}}^{\text{NO}_2}$  are the reactions involving  $\text{NO}_2$  with apoplastic ascorbate and nitrate reductase (Eller and Sparks, 2006; Teklemarian and Sparks, 2006; Hu and Sun, 2010). The higher are the concentrations of ascorbate and nitrate reductance, the higher is the depletion of  $\text{NO}_2$  in the sub-stomatal cavity and the lower is  $R_{\text{int}}^{\text{NO}_2}$ . However, these reactions are irreversible and ascorbate and nitrate reductance are not immediately regenerated. Thus, the dynamics of  $R_{\text{int}}^{\text{NO}_2}$  and its contribution to the total leaf resistance probably reflect these biological processes: the pool of apoplastic ascorbate and nitrate reductase progressively decreased during the morning due to the reactions with  $\text{NO}_2$ , leading to the increase of  $R_{\text{int}}^{\text{NO}_2}$  in the afternoon. Since these substances are not regenerated immediately,  $R_{\text{int}}^{\text{NO}_2}$  remained at its maximal value during the afternoon. Finally, during  
15 nighttime when stomatal closure prevented  $\text{NO}_2$  to enter into the sub-stomatal cavity (and thus did not react with apoplastic ascorbate and nitrate reductase), the pool of ascorbate and nitrate reductase was regenerated leading to minimal  $R_{\text{int}}^{\text{NO}_2}$  values in the morning.

## BGD

10, 4461–4514, 2013

### Measurements of nitrogen oxides and ozone fluxes

P. Stella et al.

Title Page

Abstract

Introduction

Conclusions

References

Tables

Figures

⏪

⏩

◀

▶

Back

Close

Full Screen / Esc

Printer-friendly Version

Interactive Discussion



## 4 Conclusions

This study reports about measurements of NO, NO<sub>2</sub> and O<sub>3</sub> surface-atmosphere exchange fluxes using the eddy covariance method. This is a direct method to measure exchange fluxes without disturbance of the micrometeorological conditions and thus without impacts on plant functioning. The experiment was carried out during the SALSA campaign over a meadow in Southern Germany from 29 August to 20 September 2005.

Initially, our a priori NO<sub>2</sub> deposition fluxes modelled with the Surf atm model have not considered any internal resistance. In this case, the modelled NO<sub>2</sub> deposition flux exceeded the measured NO<sub>2</sub> deposition flux by a factor of two. In order to identify the processes responsible for this overestimation, (i) the influence of a chemical divergence above the canopy, (ii) the existence of an NO<sub>2</sub> emission flux from vegetation, (iii) the potential underestimation of the resistances used in the model, and (iv) the existence of the internal resistance for NO<sub>2</sub> were explored.

The results did not suggest a considerable influence of chemical reactions above (and within) the canopy. In addition, the non-existence of a canopy compensation point for NO<sub>2</sub> excluded the presence of an NO<sub>2</sub> emission flux from vegetation. Moreover, the sensitivity of the model to the soil resistance to NO<sub>2</sub> only accounted for a small difference between measured and modelled flux, which was 13 % during daytime if the soil deposition was assumed to be zero. The other resistances were implicitly validated owing to the good agreement between measured and modelled O<sub>3</sub> fluxes.

Consequently, only the existence of an internal resistance limiting NO<sub>2</sub> stomatal uptake could explain the overestimation by the Surf atm model. The median internal resistance for NO<sub>2</sub> was estimated from the NO<sub>2</sub> flux measurements and from the modelled resistances, to be about 300 sm<sup>-1</sup>, while the median for the stomatal resistance was only around 100 sm<sup>-1</sup> during daytime. Consequently, the internal resistance represented between 50 % and 90 % of the total leaf resistance.

This study proved the existence of a large and significant internal resistance for NO<sub>2</sub> for the grass species present at the meadow. For the first time, this type of

BGD

10, 4461–4514, 2013

### Measurements of nitrogen oxides and ozone fluxes

P. Stella et al.

Title Page

Abstract

Introduction

Conclusions

References

Tables

Figures



Back

Close

Full Screen / Esc

Printer-friendly Version

Interactive Discussion



investigation was made without an alteration of the microclimatological conditions that may occur when using the chamber method. This topic is particularly relevant for estimating dry deposition of NO<sub>2</sub> over terrestrial ecosystems. An internal resistance is currently not taken into account in global models such as the EMEP model (Tsyro, 2001; Simpson et al., 2003), the MOZART model (Horovitz et al., 2003), or strongly underestimated such as in the MATCH-MPIC model, in which the internal resistance is assumed to be the half of the leaf stomatal resistance (Ganzeveld and Lelieveld, 1995; Shepon et al., 2007). These issues could lead to a large overestimation of the terrestrial NO<sub>2</sub> sink. Nevertheless, further studies at other ecosystems are required to establish a parameterisation of the internal resistance as a function of land use that can be implemented in global chemistry and transport models.

The service charges for this open access publication have been covered by the Max Planck Society.

*Acknowledgements.* The authors gratefully acknowledge financial support by the German Research Foundation (DFG project SALSA, ME 2100/1-1) and by the Max Planck Society. We are indebted to the German Meteorological Service (DWD) for a fruitful collaboration. We thank Mr. Graf (owner of the meadow), A. Thielmann, M. Welling, V. Wolff, K. Staudt, L. Pfannkuch, M. Scheibe and family Schindler for their help and support during the field measurements.

## References

- Ainsworth, E. A.: Rice production in a changing climate: a meta-analysis of responses to elevated carbon dioxide and elevated ozone concentration, *Glob. Change. Biol.*, 14, 1642–1650, 2008.
- Almeida, E., Marracos, M., Morcillo, M., and Rosales, B.: Atmospheric corrosion of mild steel, Part I: Rural and urban atmosphere, *Mater. Corros.*, 51, 859–864, 2000.
- Altimir, N., Kolari, P., Tuovinen, J.-P., Vesala, T., Bäck, J., Suni, T., Kulmala, M., and Hari, P.: Foliage surface ozone deposition: a role for surface moisture?, *Biogeosciences*, 3, 209–228, doi:10.5194/bg-3-209-2006, 2006.

## Measurements of nitrogen oxides and ozone fluxes

P. Stella et al.

Title Page

Abstract

Introduction

Conclusions

References

Tables

Figures



Back

Close

Full Screen / Esc

Printer-friendly Version

Interactive Discussion



## Measurements of nitrogen oxides and ozone fluxes

P. Stella et al.

Title Page

Abstract

Introduction

Conclusions

References

Tables

Figures

◀

▶

◀

▶

Back

Close

Full Screen / Esc

Printer-friendly Version

Interactive Discussion



- Atkinson, R., Baulch, D. L., Cox, R. A., Crowley, J. N., Hampson, R. F., Hynes, R. G., Jenkin, M. E., Rossi, M. J., and Troe, J.: Evaluated kinetic and photochemical data for atmospheric chemistry: Volume I – gas phase reactions of O<sub>x</sub>, HO<sub>x</sub>, NO<sub>x</sub> and SO<sub>x</sub> species, *Atmos. Chem. Phys.*, 4, 1461–1738, doi:10.5194/acp-4-1461-2004, 2004.
- 5 Aubinet, M., Grelle, A., Ibrom, A., Rannik, U., Moncrieff, J., Foken, T., Kowalski, A. S., Martin, P. H., Berbigier, P., Bernhofer, C., Clement, R., Elbers, J., Granier, A., Grunwald, T., Morgenstern, K., Pilegaard, K., Rebmann, C., Snijders, W., Valentini, R., and Vesala, T.: Estimates of the annual net carbon and water exchange of forests: the EUROFLUX methodology, *Adv. Ecol. Res.*, 30, 113–175, 2000.
- 10 Aubinet, M., Vesala, T., and Papale, D.: *Eddy Covariance: a Practical Guide to Measurement and Data Analysis*, Springer, Dordrecht, Heidelberg, London, New York, 438 pp., 2012.
- Avnery, S., Mauzerall, D. L., Liu, J., and Horowitz, L. W.: Global crop yield reductions due to surface ozone exposure: 1. Year 2000 crop production losses and economic damage, *Atmos. Environ.*, 45, 2284–2296, 2011a.
- 15 Avnery, S., Mauzerall, D. L., Liu, J., and Horowitz, L. W.: Global crop yield reductions due to surface ozone exposure: 2. Year 2030 potential crop production losses and economic damage under two scenarios of O<sub>3</sub> pollution, *Atmos. Environ.*, 45, 2297–2309, 2011b.
- Baldocchi, D. D., Falge, E., Gu, L., Olson, R., Hollinger, D., Running, S., Anthoni, P., Bernhofer, C., Davis, K., Evans, R., Fuentes, J., Goldstein, A., Katul, G., Law, B., Lee, X., Malhi, Y., Meyers, T., Munger, W., Oechel, W., Paw U, K. T., Pilegaard, K., Schmid, H. P., Valentini, R., Verma, S., Vesala, T., Wilson, K., and Wofsy, S.: FLUXNET: a new tool to study the temporal and spatial variability of ecosystem-scale carbon dioxide, water vapor and energy flux densities, *B. Am. Meteorol. Soc.*, 82, 2415–2434, 2001.
- 20 Bargsten, A., Falge, E., Pritsch, K., Huwe, B., and Meixner, F. X.: Laboratory measurements of nitric oxide release from forest soil with a thick organic layer under different understory types, *Biogeosciences*, 7, 1425–1441, doi:10.5194/bg-7-1425-2010, 2010.
- 25 Boyce, A., Nord, A. G., and Tronner, K.: Atmospheric bronze and copper corrosion as an environmental indicator, *Water. Air. Soil. Poll.*, 127, 193–205, 2001.
- Breuninger, C., Oswald, R., Kesselmeier, J., and Meixner, F. X.: The dynamic chamber method: trace gas exchange fluxes (NO, NO<sub>2</sub>, O<sub>3</sub>) between plants and the atmosphere in the laboratory and in the field, *Atmos. Meas. Tech.*, 5, 955–989, doi:10.5194/amt-5-955-2012, 2012.
- 30

**Measurements of  
nitrogen oxides and  
ozone fluxes**

P. Stella et al.

Title Page

Abstract

Introduction

Conclusions

References

Tables

Figures

◀

▶

◀

▶

Back

Close

Full Screen / Esc

Printer-friendly Version

Interactive Discussion



Burba, G. and Anderson, D.: A brief practical guide to eddy covariance flux measurements: principles and workflow examples for scientific and industrial applications, Licor, 214 pp., 2010.

Chaparro-Suarez, I. G., Meixner, F. X., and Kesselmeier, J.: Nitrogen dioxide (NO<sub>2</sub>) uptake by vegetation controlled by atmospheric concentrations and plant stomatal aperture, *Atmos. Environ.*, 45, 5742–5750, 2011.

Choudhury, B. J. and Monteith, J. L.: A four-layer model for the heat budget of homogeneous land surfaces, *Q. J. Roy. Meteor. Soc.*, 114, 373–398, 1988.

Coyle, M., Smith, R. I., Stedman, J. R., Weston, K. J., and Fowler, D.: Quantifying the spatial distribution of surface ozone concentration in the UK, *Atmos. Environ.*, 36, 1013–1024, 2002.

Crutzen, P. J.: The influence of nitrogen oxides on the atmospheric ozone content, *Q. J. Roy. Meteor. Soc.*, 96, 320–325, 1970.

Crutzen, P. J.: The role of NO and NO<sub>2</sub> in the chemistry of the troposphere and stratosphere, *Annu. Rev. Earth. Pl. Sc.*, 7, 443–472, 1979.

Crutzen, P. J.: Atmospheric interactions of homogeneous gas reaction of C, N, and S containing compounds, in: *The Major Biogeochemical Cycles and their Interactions*, edited by: Bolin, B. and Cook, R. B., Wiley, New York, 219–235, 1983.

Damköhler, G.: Der Einfluss der Turbulenz auf die Flammgeschwindigkeit in Gasgemischen, *Z. Elektrochem. Angew. P.*, 46, 601–652, 1940.

Dari-Salisburgo, C., Di Carlo, P., Giammaria, F., Kajii, Y., and D'Altorio, A.: Laser induced fluorescence instrument for NO<sub>2</sub> measurements: observations at a central Italy background site, *Atmos. Environ.*, 43, 970–977, 2009.

De Arellano, J. V. G. and Duynkerke, P. G.: Influence of chemistry on the flux-gradient relationships for the NO-O<sub>3</sub>-NO<sub>2</sub> system, *Bound.-Lay. Meteorol.*, 61, 375–387, 1992.

Delmas, R., Serça, D., and Jambert, C.: Global inventory of NO<sub>x</sub> sources, *Nutr. Cycl. Agroecosys.*, 48, 51–60, 1997.

Desjardins, R. L., Macpherson, J. I., Schuepp, P. H., and Karanja, F.: An evaluation of aircraft flux measurements of CO<sub>2</sub>, water-vapor and sensible heat, *Bound.-Lay. Meteorol.*, 47, 55–69, 1989.

Dolman, A. J., Noilhan, J., Durand, P., Sarrat, C., Brut, A., Piguet, B., Butet, A., Jarosz, N., Brunet, Y., Loustau, D., Lamaud, E., Tolk, L., Ronda, R., Miglietta, F., Gioli, B., Magliulo, V., Esposito, M., Gerbig, C., Körner, S., Glademard, P., Ramonet, M., Ciais, P., Neininger, B., Hutjes, R. W. A., Elbers, J. A., Macatangay, R., Schrems, O., Pérez-Landa, G., Sanz, M. J.,

## Measurements of nitrogen oxides and ozone fluxes

P. Stella et al.

[Title Page](#)

[Abstract](#)

[Introduction](#)

[Conclusions](#)

[References](#)

[Tables](#)

[Figures](#)

◀

▶

◀

▶

[Back](#)

[Close](#)

[Full Screen / Esc](#)

[Printer-friendly Version](#)

[Interactive Discussion](#)



Scholz, Y., Facon, G., Ceschia, E., and Beziat, P.: The CarboEurope regional experiment strategy, *B. Am. Meteorol. Soc.*, 87, 1367–1379, 2006.

Dunlea, E. J., Herndon, S. C., Nelson, D. D., Volkamer, R. M., San Martini, F., Sheehy, P. M., Zahniser, M. S., Shorter, J. H., Wormhoudt, J. C., Lamb, B. K., Allwine, E. J., Gaffney, J. S., Marley, N. A., Grutter, M., Marquez, C., Blanco, S., Cardenas, B., Retama, A., Ramos Villegas, C. R., Kolb, C. E., Molina, L. T., and Molina, M. J.: Evaluation of nitrogen dioxide chemiluminescence monitors in a polluted urban environment, *Atmos. Chem. Phys.*, 7, 2691–2704, doi:10.5194/acp-7-2691-2007, 2007.

Duyzer, J. H., Deinum, G., and Baak, J.: The interpretation of measurements of surface exchange of nitrogen oxides: correction for chemical reactions, *Philos. T. Roy. Soc. A.*, 351, 231–248, 1995.

Dyer, A. J. and Hicks, B. B.: Flux-profile relationship in the constant flux layer, *Q. J. Roy. Meteor. Soc.*, 96, 715–721, 1970.

Eller, A. S. D. and Sparks, J. D.: Predicting leaf-level fluxes of O<sub>3</sub> and NO<sub>2</sub>: the relative roles of diffusion and biochemical processes, *Plant. Cell. Environ.*, 29, 1742–1750, 2006.

Emberson, L. D., Ashmore, M. R., Cambridge, H. M., Simpson, D., and Tuovinen, J. P.: Modelling stomatal ozone flux across Europe, *Environ. Pollut.*, 109, 403–413, 2000.

Erismann, J. W., Van Pul, A., and Wyers, P.: Parameterization of surface resistance for the quantification of atmospheric deposition of acidifying pollutants and ozone, *Atmos. Environ.*, 28, 2595–2607, 1994.

Eugster, W. and Hesterberg, R.: Transfer resistances of NO<sub>2</sub> determined from eddy correlation flux measurements over a litter meadow at a rural site on the Swiss plateau, *Atmos. Environ.*, 30, 1247–1254, 1996.

Fehsenfeld, F. C., Drummond, J. W., Roychowdhury, U. K., Galvin, P. J., Williams, E. J., Buhr, M. P., Parrish, D. D., Hubler, G., Langford, A. O., Calvert, J. G., Ridley, B. A., Grahek, F., Heikes, B. G., Kok, G. L., Shetter, J. D., Walega, J. G., Elsworth, C. M., Norton, R. B., Fehney, D. W., Murphy, P. C., Hovermale, C., Mohnen, V. A., Demerjian, K. L., Mackay, G. I., and Schiff, H. I.: Intercomparison of NO<sub>2</sub> measurement techniques, *J. Geophys. Res.-Atmos.*, 95, 3579–3597, 1990.

Felzer, B. S., Cronin, T., Reilly, J. M., Melillo, J. M., and Wang, X.: Impacts of ozone on trees and crops, *C. R. Geosci.*, 339, 784–798, 2007.

Foken, T.: *Micrometeorology*, Springer Verlag, Berlin, Heidelberg, 308 pp., 2008.

## Measurements of nitrogen oxides and ozone fluxes

P. Stella et al.

[Title Page](#)

[Abstract](#)

[Introduction](#)

[Conclusions](#)

[References](#)

[Tables](#)

[Figures](#)



[Back](#)

[Close](#)

[Full Screen / Esc](#)

[Printer-friendly Version](#)

[Interactive Discussion](#)



- Foken, T. and Wichura, B.: Tools for quality assessment of surface-based flux measurements, *Agr. Forest. Meteorol.*, 78, 83–105, 1996.
- Foken, T., Göckede, M., Mauder, M., Mahrt, L., Amiro, B., and Munger, W.: Postfield data quality control, in: *Handbook of Micrometeorology: a Guide for Surface Flux Measurements and Analysis*, edited by: Lee, X., Massman, W. J., and Law, B. E., Kluwer Academic Publishers, 181–208, 2004.
- Foken, T., Aubinet, M., and Leuning R: The eddy-covariation method, in: *Eddy Covariance: a Practical Guide to Measurement and Data Analysis*, edited by: Aubinet, M., Vesala, T., and Papale, D., Springer, Dordrecht, Heidelberg, London, New York, 1–19, 2012.
- Forster, P., Ramaswamy, V., Artaxo, P., Berntsen, T., Betts, R., Fahey, D. W., Haywood, J., Lean, J., Lowe, D. C., Myhre, G., Nganga, J., Prinn, R., Raga, G., Schulz, M., and Van Dorland, R.: Changes in Atmospheric Constituents and in Radiative Forcing, in: *Climate Change 2007: The Physical Basis. Contribution of Working Group I to Fourth Assessment Report of IPCC on Climate Change*, edited by: Solomon, S., Qin, D., Manning, M., Chen, Z., Marquis, M., Averyt, K. B., Tignor, M., and Miller, H. L., Cambridge University Press, Cambridge, UK/NY, USA, 129–234, 2007.
- Fowler, D., Pilegaard, K., Sutton, M. A., Ambus, P., Raivonen, M., Duyzer, J., Simpson, D., Fagerli, H., Fuzzi, S., Schjoerring, J. K., Granier, C., Neftel, A., Isaksen, I. S. A., Laj, P., Maione, M., Monks, P. S., Burkhardt, J., Daemmgen, U., Neiryneck, J., Personne, E., Wichink-Kruit, R., Butterbach-Bahl, K., Flechard, C., Tuovinen, J. P., Coyle, M., Gerosa, G., Loubet, B., Altimir, N., Gruenhage, L., Ammann, C., Cieslik, S., Paoletti, E., Mikkelsen, T. N., Ro-Poulsen, H., Cellier, P., Cape, J. N., Horvath, L., Loreto, F., Niinemets, U., Palmer, P. I., Rinne, J., Misztal, P., Nemitz, E., Nilsson, D., Pryor, S., Gallagher, M. W., Vesala, T., Skiba, U., Brüggemann, N., Zechmeister-Boltenstern, S., Williams, J., O'Dowd, C., Facchini, M. C., de Leeuw, G., Flossman, A., Chaumerliac, N., Erisman, J. W.: Atmospheric composition change: ecosystems–atmosphere interactions, *Atmos. Environ.*, 43, 5193–5267, 2009.
- Galmarini, S., De Arellano, J. V. G., and Duyzer, J.: Fluxes of chemically reactive species inferred from mean concentration measurements, *Atmos. Environ.*, 31, 2371–2374, 1997.
- Ganzeveld, L. and Lelieveld, J.: Dry deposition parameterization in a chemistry general circulation model and its influence on the distribution of reactive trace gases, *J. Geophys. Res.*, 100, 20999–21012, doi:10.1029/95JD02266, 1995.
- Garland, J. A.: The dry deposition of sulphur dioxide to land and water surface, *P. R. Soc. Lond. A-Conta.*, 354, 245–268, 1997.

## Measurements of nitrogen oxides and ozone fluxes

P. Stella et al.

Title Page

Abstract

Introduction

Conclusions

References

Tables

Figures



Back

Close

Full Screen / Esc

Printer-friendly Version

Interactive Discussion

Geßler, A., Rienks, M., and Rennenberg, H.: NH<sub>3</sub> and NO<sub>2</sub> fluxes between beech trees and the atmosphere – correlation with climatic and physiological parameters, *New. Phytol.*, 147, 539–560, 2000.

Geßler, A., Rienks, M., and Rennenberg, H.: Stomatal uptake and cuticular adsorption contribute to dry deposition of NH<sub>3</sub> and NO<sub>2</sub> to needles of adult spruce (*Picea abies*) trees, *New. Phytol.*, 156, 179–194, 2002.

Gerosa, G., Marzuoli, R., Cieslik, S., and Ballarin-Denti, A.: Stomatal ozone fluxes over barley field in Italy, “Effective exposure” as a possible link between exposure- and flux-based approaches, *Atmos. Environ.*, 38, 2421–2432, 2004.

Göckede, M., Rebmann, C., and Foken, T.: A combination of quality assessment tools for eddy covariance measurements with footprint modelling for the characterisation of complex sites, *Agr. Forest. Meteorol.*, 127, 175–188, 2004.

Göckede, M., Markkanen, T., Hasager, C. B., and Foken, T.: Update of a footprint-based approach for the characterisation of complex measuring sites, *Bound.-Lay. Meteorol.*, 118, 635–655, 2006.

Güsten, H. and Heinrich, G.: On-line measurements of ozone surface fluxes: Part I. Methodology and instrumentation, *Atmos. Environ.*, 30, 897–909, 1996.

Güsten, H., Heinrich, G., Schmidt, R. W. H., and Schurath, U.: A novel ozone sensor for direct eddy flux measurements, *J. Atmos. Chem.*, 14, 73–84, 1992.

Gut, A., Scheibe, M., Rottenberger, S., Rummel, U., Welling, M., Ammann, C., Kirkman, G. A., Kuhn, U., Meixner, F. X., Kesselmeier, J., Lehmann, B. E., Schmidt, W., Müller, E., and Piedade, M. T. F.: Exchange fluxes of NO<sub>2</sub> and O<sub>3</sub> at soil and leaf surfaces in an Amazonian rain forest, *J. Geophys. Res.*, 107, 8060, doi:10.1029/2001JD000654, 2002.

Hazucha, M. J. and Lefohn, A. S.: Nonlinearity in human health response to ozone: experimental laboratory considerations, *Atmos. Environ.*, 41, 4559–4570, 2007.

Hereid, D. P. and Monson, R. K.: Nitrogen oxide fluxes between corn (*Zea mays* L.) leaves and the atmosphere, *Atmos. Environ.*, 35, 975–983, 2001.

Hicks, B. B., Baldocchi, D. D., Meyers, T. P., Hosker Jr., R. P., and Matt, D. R.: A preliminary multiple resistance routine for deriving dry deposition velocities from measured quantities, *Water. Air. Soil. Pollut.*, 36, 311–330, 1987.

Hillstrom, M. L. and Lindroth, R. L.: Elevated atmospheric carbon dioxide and ozone alter forest insect abundance and community composition, *Insect. Conserv. Diver.*, 1, 233–241, 2008.

## Measurements of nitrogen oxides and ozone fluxes

P. Stella et al.

Title Page

Abstract

Introduction

Conclusions

References

Tables

Figures

◀

▶

◀

▶

Back

Close

Full Screen / Esc

Printer-friendly Version

Interactive Discussion



- Horowitz, L., Walters, S., Mauzerall, D. L., Emmons, L. K., Rasch, P. J., Granier, C., Tie, X., Lamarque, J- F., Schultz, M. G., Tyndall, G. S., Orlando, J. J., and Brasseur, G. P.: A global simulation of tropospheric ozone and related tracers: description and evaluation of MOZART, version 2, *J. Geophys. Res.*, 108, 4784, doi:10.1029/2002JD002853, 2003.
- 5 Hosaynali Beygi, Z., Fischer, H., Harder, H. D., Martinez, M., Sander, R., Williams, J., Brookes, D. M., Monks, P. S., and Lelieveld, J.: Oxidation photochemistry in the Southern Atlantic boundary layer: unexpected deviations of photochemical steady state, *Atmos. Chem. Phys.*, 11, 8497–8513, doi:10.5194/acp-11-8497-2011, 2011.
- Hu, Y. and Sun., G.: Leaf nitrogen dioxide uptake coupling apoplastic chemistry, carbon/sulphur assimilation, and plant nitrogen status, *Plant. Cell. Rep.*, 29, 1069–1077, 2010.
- 10 Johansson, C.: Pine forest: a negligible sink for atmospheric  $\text{NO}_x$  in rural Sweden, *Tellus B*, 39, 426–438, 1987.
- Kley, D. and McFarland, M.: Chemiluminescence detector for NO and  $\text{NO}_2$ , *Atmos. Technol.*, 12, 63–69, 1980.
- 15 Kowalski, S., Sartore, M., Burlett, R., Berbigier, P., and Loustau, D.: The annual carbon budget of a French pine forest (*Pinus Pinaster*) following harvest, *Glob. Change. Biol.*, 9, 1051–1065, 2003.
- Kowalski, S., Loustau, D., Berbigier, P., Manca, G., Tedeschi, V., Borghetti, M., Valentini, R., Kolari, P., Berniger, F., Rannik, U., Hari, P., Rayment, M., Mencuccini, M., Moncrieff, J., and Grace, J.: Paired comparison of carbon exchange between undisturbed and regenerating stands in four managed forests in Europe, *Glob. Change. Biol.*, 10, 1707–1723, 2004.
- 20 Kramm, G., Müller, H., Fowler, D., Höfken, K., Meixner, F. X., and Schaller, E.: A modified profile method for determining the vertical fluxes of NO,  $\text{NO}_2$ , Ozone, and  $\text{HNO}_3$  in the atmospheric surface layer, *J. Atmos. Chem.*, 13, 265–288, 1991.
- 25 Kramm, G., Beier, N., Foken, T., Müller, H., Schröder, P., and Seiler, W.: A SVAT Scheme for NO,  $\text{NO}_2$  and  $\text{O}_3$  – model description and test results, *Meteorol. Atmos. Phys.*, 61, 89–106, 1996.
- Lamaud, E., Loubet, B., Irvine, M., Stella, P., Personne, E., and Cellier, P.: Partitioning of ozone deposition over a developed maize crop between stomatal and non-stomatal uptakes, using eddy-covariance flux measurements and modelling, *Agr. Forest. Meteorol.*, 149, 1385–1386, 2009.
- 30

## Measurements of nitrogen oxides and ozone fluxes

P. Stella et al.

Title Page

Abstract

Introduction

Conclusions

References

Tables

Figures

◀

▶

◀

▶

Back

Close

Full Screen / Esc

Printer-friendly Version

Interactive Discussion



Laville, P., Flura, D., Gabrielle, B., Loubet, B., Fanucci, O., Rolland, M. N., and Cellier, P.: Characterisation of soil emissions of nitric oxide at field and laboratory scale using high resolution method, *Atmos. Environ.*, 43, 2648–2658, 2009.

Lerdau, M. T., Munger, J. W., and Jacob, D. J.: The NO<sub>2</sub> flux conundrum, *Science*, 289, 2291–2293, 2000.

Lenschow, D. H.: Reactive trace species in the boundary layer from a micrometeorological perspective, *J. Meteorol. Soc. Jpn.*, 60, 472–480, 1982.

Lenschow, D. H. and Delany, A. C.: An analytic formulation for NO and NO<sub>2</sub> flux profiles in the atmospheric surface layer, *J. Atmos. Chem.*, 5, 301–309, 1987.

Loubet, B., Cellier, P., Milford, C., and Sutton, M. A.: A coupled dispersion and exchange model for short-range dry deposition of atmospheric ammonia, *Q. J. Roy. Meteor. Soc.*, 132, 1733–1763, 2006.

Levy, J. I., Chemerynski, S. M., and Sarnat, J. A.: Ozone exposure and mortality: an empiric Bayes metaregression analysis, *Epidemiology*, 16, 458–468, 2005.

Ludwig, J., Meixner, F. X., Vogel, B., Förstner, J.: Soil-air exchange of nitric oxide: an overview of processes, environmental factors, and modelling studies, *Biogeochemistry*, 52, 225–257, 2001.

Massman, W. J.: A review of the molecular diffusivities of H<sub>2</sub>O, CO<sub>2</sub>, CH<sub>4</sub>, CO, O<sub>3</sub>, SO<sub>2</sub>, NH<sub>3</sub>, N<sub>2</sub>O, NO and NO<sub>2</sub> in air, O<sub>2</sub> and N<sub>2</sub> near STP, *Atmos. Environ.*, 32, 1111–1127, 1998.

Massman, W. J.: Toward an ozone standard to protect vegetation based on effective dose: a review of deposition resistances and possible metric, *Atmos. Environ.*, 38, 2323–2337, 2004.

Massman, W. J. and Lee, X.: Eddy covariance flux corrections and uncertainties in long-term studies of carbon and energy exchanges, *Agr. Forest. Meteorol.*, 113, 121–144, 2002.

Mayer, J.-C., Staudt, K., Gilge, S., Meixner, F. X., and Foken, T.: The impact of free convection on late morning ozone decreases on an Alpine foreland mountain summit, *Atmos. Chem. Phys.*, 8, 5941–5956, doi:10.5194/acp-8-5941-2008, 2008.

Mayer, J. C., Bargsten, A., Rummel, U., Meixner, F. X., and Foken, T.: Distributed modified Bowen ratio method for surface layer fluxes of reactive and non-reactive trace gases, *Agr. Forest. Meteorol.*, 151, 655–668, 2011.

Meixner, F. X.: Surface exchange of odd nitrogen oxides, *Nova Act. Lc.*, 70, 299–348, 1994.

## Measurements of nitrogen oxides and ozone fluxes

P. Stella et al.

[Title Page](#)

[Abstract](#)

[Introduction](#)

[Conclusions](#)

[References](#)

[Tables](#)

[Figures](#)

◀

▶

◀

▶

[Back](#)

[Close](#)

[Full Screen / Esc](#)

[Printer-friendly Version](#)

[Interactive Discussion](#)



Meixner, F. X., Fickinger, Th., Marufu, L., Serca, D., Nathaus, F. J., Makina, E., Mukurumbira, L., and Andreae, M. O.: Preliminary results on nitric oxide emission from a southern African savanna ecosystem, *Nutr. Cycl. Agroecosys.*, 48, 123–138, 1997.

Monteith, J. L.: Evaporation and surface temperature, *Q. J. Roy. Meteor. Soc.*, 107, 1–27, 1981.

Muller, J. B. A., Percival, C. J., Gallagher, M. W., Fowler, D., Coyle, M., and Nemitz, E.: Sources of uncertainty in eddy covariance ozone flux measurements made by dry chemiluminescence fast response analysers, *Atmos. Meas. Tech.*, 3, 163–176, doi:10.5194/amt-3-163-2010, 2010.

Oncley, S. P.: Flux Parameterization Techniques in the Atmospheric Surface Layer, Dissertation at the University of California, Irvine, CA, 202 pp., 1989.

Paoletti, E.: Ozone slows stomatal response to light and leaf wounding in a Mediterranean evergreen broadleaf, *Arbustus unedo*, *Environ. Pollut.*, 134, 439–445, 2005.

Pape, L., Ammann, C., Nyfeler-Brunner, A., Spirig, C., Hens, K., and Meixner, F. X.: An automated dynamic chamber system for surface exchange measurement of non-reactive and reactive trace gases of grassland ecosystems, *Biogeosciences*, 6, 405–429, doi:10.5194/bg-6-405-2009, 2009.

Parrish, D. D. and Fensfeld, F. C.: Methods for gas-phase measurements of ozone, ozone precursors and aerosol precursors, *Atmos. Environ.*, 34, 1921–1957, 2000.

Payne, R. J., Stevens, C. J., Dise, N. B., Gowing, D. J., Pilkington, M. G., Phoenix, G. K., Emmett, B. A., and Ashmore, M. R.: Impacts of atmospheric pollution on the plant communities of British acid grasslands, *Environ. Pollut.*, 159, 2602–2608, 2011.

Personne, E., Loubet, B., Herrmann, B., Mattsson, M., Schjoerring, J. K., Nemitz, E., Sutton, M. A., and Cellier, P.: SURFATM-NH<sub>3</sub>: a model combining the surface energy balance and bi-directional exchanges of ammonia applied at the field scale, *Biogeosciences*, 6, 1371–1388, doi:10.5194/bg-6-1371-2009, 2009.

Pilegaard, K., Hummelshoj, P., and Jensen, N. O.: Fluxes of ozone and nitrogen dioxide measured by eddy correlation over a harvested wheat field, *Atmos. Environ.*, 32, 1167–1177, 1998.

Pollack, I. B., Lerner, B. M., and Ryerson, T. B.: Evaluation of ultraviolet light-emitting diodes for detection of atmospheric NO<sub>2</sub> by photolysis – chemiluminescence, *J. Atmos. Chem.*, 65, 111–125, 2011.

Raupach, M. R., Finnigan, J. J., and Brunet, Y.: Coherent eddies and turbulence inside vegetation canopies. The mixing layer analogy, *Bound.-Lay. Meteorol.*, 78, 351–382, 1996.

## Measurements of nitrogen oxides and ozone fluxes

P. Stella et al.

Title Page

Abstract

Introduction

Conclusions

References

Tables

Figures

◀

▶

◀

▶

Back

Close

Full Screen / Esc

Printer-friendly Version

Interactive Discussion



- Remde, A. and Conrad, R.: Role of nitrification and denitrification for NO metabolism in soil, *Biogeochemistry*, 12, 189–205, 1991.
- Remde, A., Slemr, F., and Conrad, R.: Microbial production and uptake of nitric oxide in soil, *FEMS. Microbiol. Ecol.*, 62, 221–230, 1989.
- 5 Remde, A., Ludwig, J., Meixner, F. X., and Conrad, R.: A study to explain the emission of nitric oxide from a marsh soil, *J. Atmos. Chem.*, 17, 249–275, 1993.
- Ridley, B. A., Carroll, M. A., Torres, A. L., Condon, E. P., Sachse, G. W., Hill, G. F., and Gregory, G. L.: An intercomparison of results from ferrous sulfate and photolytic converter techniques for measurements of No-Chi Made during the Nasa Gte Cite-1 Aircraft Program, *J. Geophys. Res.-Atmos.*, 93, 15803–15811, 1988.
- 10 Rondón, A., Johansson, C., and Granat, L.: Dry deposition of nitrogen dioxide and ozone to coniferous forests, *J. Geophys. Res.*, 98, 5159–5172, 1993.
- Rummel, U., Ammann, C., Kirkman, G. A., Moura, M. A. L., Foken, T., Andreae, M. O., and Meixner, F. X.: Seasonal variation of ozone deposition to a tropical rain forest in southwest Amazonia, *Atmos. Chem. Phys.*, 7, 5415–5435, doi:10.5194/acp-7-5415-2007, 2007.
- Running, S. W., Baldocchi, D. D., Turner, D. P., Gower, S. T., Bakwin, P. S., and Hibbard, K. A.: A global terrestrial monitoring network integrating tower fluxes, flask sampling, ecosystem modelling and EOS satellite data, *Remote. Sens. Environ.*, 70, 108–127, 1999.
- Segschneider, H. J., Wildt, J., and Förstel, H.: Uptake of  $^{15}\text{NO}_2$  by sunflower (*Helianthus annuus*) during exposures in light and darkness: quantities, relationship to stomatal aperture and incorporation into different nitrogen pools within the plant, *New. Phytol.*, 131, 109–119, 1995.
- 20 Shepon, A., Gildor, H., Labrador, L. J., Butler, T., Ganzeveld, L. N., and Lawrence, M. G.: Global reactive nitrogen deposition from lightning  $\text{NO}_x$ , *J. Geophys. Res.*, 112, D06304, doi:10.1029/2006JD007458, 2007.
- Shuttleworth, W. J. and Wallace, S. J.: Evaporation from sparse crop – an energy combination theory, *Q. J. Roy. Meteor. Soc.*, 111, 477–507, 1985.
- Simpson, D., Fagerli, H., Jonson, J., Tsyro, S., Wind, P., and Tuovinen, J. P.: The EMEP Unified Eulerian Model. Model Description, EMEP MSC-W Report 1/2003, The Norwegian Meteorological Institute, Oslo, Norway, 2003.
- 30 Sitch, S., Cox, P. M., Collins, W. J., and Huntingford, C.: Indirect radiative forcing of climate change through ozone effects on the land-carbon sink, *Nature*, 448, 791–795, 2007.

## Measurements of nitrogen oxides and ozone fluxes

P. Stella et al.

Title Page

Abstract

Introduction

Conclusions

References

Tables

Figures



Back

Close

Full Screen / Esc

Printer-friendly Version

Interactive Discussion



- Skiba, U., Drewer, J., Tang, Y. S., van Dijk, N., Helfter, C., Nemitz, E., Famulari, D., Cape, J. N., Jones, S. K., Twigg, M., Pihlatie, M., Vesala, T., Larsen, K. S., Carter, M. S., Ambus, P., Ibrom, A., Beier, C., Hensen, A., Frumau, A., Erisman, J. W., Brüggemann, N., Gasche, R., Butterbach-Bahl, K., Neftel, A., Spirig, C., Horvath, L., Freibauer, A., Cellier, P., Laville, P., Loubet, B., Magliulo, E., Bertolini, T., Seufert, G., Andersson, M., Manca, G., Laurila, T., Aurela, M., Lohila, A., Zechmeister-Boltenstern, S., Kitzler, B., Schauffler, G., Siemens, J., Kindler, R., Flechard, C., and Sutton, M. A.: Biosphere-atmosphere exchange of reactive nitrogen and greenhouse gases at the NitroEurope core flux measurements sites: measurement strategy and first data sets, *Agr. Ecosyst. Environ.*, 133, 139–149, 2009.
- Sparks, J. P., Monson, R. K., Sparks, K. L., and Lerdau, M. L.: Leaf uptake of nitrogen dioxide ( $\text{NO}_2$ ) in a tropical wet forest: implications for tropospheric chemistry, *Oecologia*, 127, 214–221, 2001.
- Spirig, C., Neftel, A., Ammann, C., Dommen, J., Grabmer, W., Thielmann, A., Schaub, A., Beauchamp, J., Wisthaler, A., and Hansel, A.: Eddy covariance flux measurements of biogenic VOCs during ECHO 2003 using proton transfer reaction mass spectrometry, *Atmos. Chem. Phys.*, 5, 465–481, doi:10.5194/acp-5-465-2005, 2005.
- Stella, P., Loubet, B., Lamaud, E., Laville, P., and Cellier, P.: Ozone deposition onto bare soil: a new parameterisation, *Agr. Forest. Meteorol.*, 151, 669–681, 2011a.
- Stella, P., Personne, E., Loubet, B., Lamaud, E., Ceschia, E., Béziat, P., Bonnefond, J. M., Irvine, M., Keravec, P., Mascher, N., and Cellier, P.: Predicting and partitioning ozone fluxes to maize crops from sowing to harvest: the Surf atm- $\text{O}_3$  model, *Biogeosciences*, 8, 2869–2886, doi:10.5194/bg-8-2869-2011, 2011b.
- Stella, P., Loubet, B., Laville, P., Lamaud, E., Cazaunau, M., Laufs, S., Bernard, F., Grosselin, B., Mascher, N., Kurtenbach, R., Mellouki, A., Kleffmann, J., and Cellier, P.: Comparison of methods for the determination of  $\text{NO}-\text{O}_3-\text{NO}_2$  fluxes and chemical interactions over a bare soil, *Atmos. Meas. Tech.*, 5, 1241–1257, doi:10.5194/amt-5-1241-2012, 2012.
- Stull, R. B.: *An Introduction to Boundary Layer Meteorology*, vol. 1, Kluwer Academic Publishers, Dordrecht, The Netherlands, 1989.
- Teklemariam, T. A. and Sparks, J. P.: Leaf fluxes of  $\text{NO}$  and  $\text{NO}_2$  in four herbaceous plant species: the role of ascorbic acid, *Atmos. Environ.*, 40, 2235–2244, 2006.
- Trebs, I., Bohn, B., Ammann, C., Rummel, U., Blumthaler, M., Königstedt, R., Meixner, F. X., Fan, S., and Andreae, M. O.: Relationship between the  $\text{NO}_2$  photolysis frequency and the solar global irradiance, *Atmos. Meas. Tech.*, 2, 725–739, doi:10.5194/amt-2-725-2009, 2009.

## Measurements of nitrogen oxides and ozone fluxes

P. Stella et al.

Title Page

Abstract

Introduction

Conclusions

References

Tables

Figures



Back

Close

Full Screen / Esc

Printer-friendly Version

Interactive Discussion



- Tsyro, S.: Description of the Lagrangian Acid Deposition Model, Technical report, EMEP, 2001.
- Vickers, D. and Mahrt, L.: Quality control and flux sampling problems for tower and aircraft data, *J. Atmos. Ocean. Tech.*, 14, 512–526, 1997.
- Walton, S., Gallagher, M. W., and Duyzer, J. H.: Use of a detailed model to study the exchange of  $\text{NO}_x$  and  $\text{O}_3$  above and below a deciduous canopy, *Atmos. Environ.*, 31, 2915–2931, 1997.
- Warneck, P.: Chemistry of the Natural Atmosphere, 2nd edn., International Geophysics Series, Academic Press Inc., San Diego, USA, 2000.
- Webb, E. K., Pearman, G. I., and Leuning, R.: Correction of flux measurements for density effects due to heat and water-vapor transfer, *Q. J. Roy. Meteor. Soc.*, 106, 85–100, 1980.
- Weber, P. and Rennenberg, H.: Dependency of nitrogen dioxide ( $\text{NO}_2$ ) fluxes to wheat (*Triticum aestivum* L.) leaves from  $\text{NO}_2$  concentration, light intensity, temperature and relative humidity determined from controlled dynamic chamber experiments, *Atmos. Environ.*, 30, 3001–3009, 1996.
- Wesely, M. L.: Parameterization of surface resistances to gaseous dry deposition in regional-scale numerical models, *Atmos. Environ.*, 23, 1293–1304, 1989.
- Wesely, M. L. and Hicks, B. B.: A review of the current status of knowledge on dry deposition, *Atmos. Environ.*, 34, 2261–2282, 2000.
- Wilczak, J. M., Oncley, S. P., and Stage, S. A.: Sonic anemometer tilt correction algorithms, *Bound.-Lay. Meteorol.*, 99, 127–150, 2001.
- Zhang, L., Brook, J. R., and Vet, R.: On ozone dry deposition with emphasis on non-stomatal uptake and wet canopies, *Atmos. Environ.*, 36, 4787–4799, 2002.

## Measurements of nitrogen oxides and ozone fluxes

P. Stella et al.

[Title Page](#)

[Abstract](#)

[Introduction](#)

[Conclusions](#)

[References](#)

[Tables](#)

[Figures](#)

⏪

⏩

◀

▶

[Back](#)

[Close](#)

[Full Screen / Esc](#)

[Printer-friendly Version](#)

[Interactive Discussion](#)



**Table 1.** Overview of stations and instrumentation used during the SALSA experiment.

Quantity	Station	Heights [m]	Instrumentation
Global radiation	MET 1 (UBT)	2.0	pyranometer CM21, Kipp & Zonen B.V., Netherlands
Net radiation	MET 2 (MPIC)	2.0	Net radiometer NR Lite, Kipp & Zonen B.V., Netherlands
$J_{\text{NO}_2}$	MET 2 (MPIC)	2.0	filter radiometer, Meteorologie Consult GmbH, Königstein, Germany
Relative humidity	MET 2 (MPIC)	2.0	Hygromer <sup>®</sup> IN-1 and Pt100 in aspirated housing, Rotronic Messgeräte GmbH, Germany
Air temperature	MET 2 (MPIC)	0.05, 0.2, 0.5, 1.0, 1.5, 2.0, 2.5, 3.0	fine-wire thermocouples; 1 Hz time resolution, Campbell Scientific, UK
Wind speed	MET 2 (MPIC)	0.2, 0.5, 1.0, 3.0	Vaisala, ultrasonic wind sensor WS425, Finland
Wind Direction	MET 2 (MPIC)	0.2, 0.5, 1.0, 3.0	Vaisala, ultrasonic wind sensor WS425, Finland
Rainfall	MET 2 (MPIC)	2.0	tipping rain gauge, ARG 100-EC, Campbell Scientific, UK
Soil temperature	MET 1 (UBT)	−0.02	TDR sonde, IMKO, Germany
Soil water content	MET 2 (MPIC)	−0.05	TDR sonde, IMKO, Germany
NO-NO <sub>2</sub> -O <sub>3</sub> mixing ratio profile	PROFILE (MPIC)	0.05, 0.20 (0.28), 0.50, 1.0, 1.65, 3.0	CLD 780TR, EcoPhysics, Switzerland Blue Light converter, BLC, Droplet Measurement Technologies Inc., USA UV absorption instrument, 49 C, Thermo Environment, USA
Momentum flux	EC 1 (UBT)	2.0	Sonic anemometer, CSAT3, Campbell Scientific, UK
Sensible heat flux			Open path gas analyzer, IRGA 7500, LiCor, USA
Latent heat flux			
CO <sub>2</sub> flux			
NO-NO <sub>2</sub> -O <sub>3</sub> fluxes	EC 2 (MPIC)	2.0	Sonic anemometer, Solent Wind Master R2, Gill Instruments, UK CLD 790SR-2, EcoPhysics, Switzerland Blue Light converter, BLC, Droplet Measurement Technologies Inc, USA OS-G2, GEFAS GmbH, Germany

## Measurements of nitrogen oxides and ozone fluxes

P. Stella et al.

**Table 2.** Comparison of measured and modelled  $\text{NO}_2$  fluxes for different values of the internal resistance. Only data for  $1/R_s^{\text{NO}_2} > 0.2 \text{ cm s}^{-1}$  ( $R_s^{\text{NO}_2} < 500 \text{ s m}^{-1}$ ) were included.

$R_{\text{int}}^{\text{NO}_2}$ ( $\text{s m}^{-1}$ )	50	100	150	200	250	300	350	400	450	500
Slope of the regression	1.19	0.94	0.79	0.70	0.63	0.57	0.53	0.50	0.47	0.44
RMSE ( $\text{nmol m}^{-2} \text{ s}^{-1}$ )	0.33	0.23	0.21	0.22	0.23	0.25	0.26	0.27	0.28	0.29

Title Page

Abstract

Introduction

Conclusions

References

Tables

Figures

◀

▶

◀

▶

Back

Close

Full Screen / Esc

Printer-friendly Version

Interactive Discussion



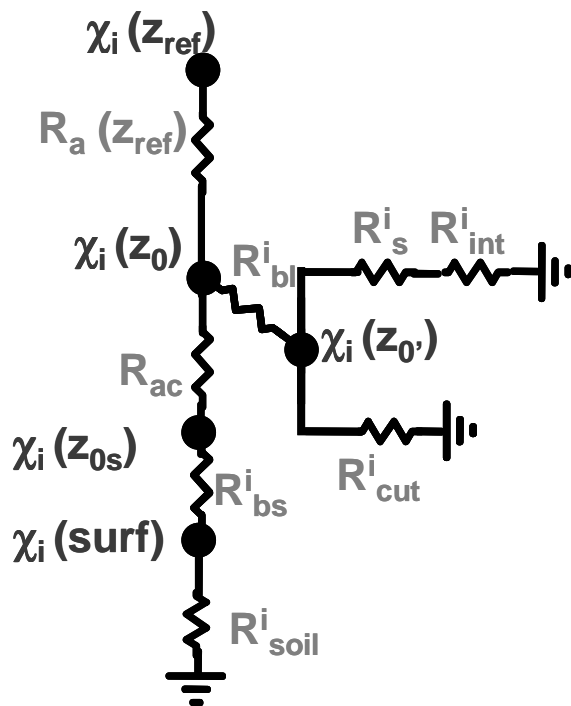


**Fig. 1.** Resistive scheme used in the Surf atm model for pollutant exchange.  $\chi$  is the gas concentration.  $R_a$ ,  $R_{ac}$ ,  $R_{bl}$ ,  $R_{bs}$ ,  $R_s$ ,  $R_{int}$ ,  $R_{cut}$  and  $R_{soil}$  are aerodynamic resistance above the canopy, aerodynamic resistance within the canopy, leaf quasi-laminar boundary layer resistance, soil quasi-laminar boundary layer resistance, stomatal resistance, internal resistance, cuticular resistance and soil resistance, respectively. Indexes  $i$ ,  $z_{ref}$ ,  $z_0$ ,  $z_{0'}$ ,  $z_{0s}$  and surf indicate the gas considered, the reference height, the canopy roughness height for momentum, the canopy roughness height for scalar, the soil roughness height for momentum, and the soil surface, respectively.

Title Page

Abstract

Introduction

Conclusions

References

Tables

Figures

◀

▶

◀

▶

Back

Close

Full Screen / Esc

Printer-friendly Version

Interactive Discussion



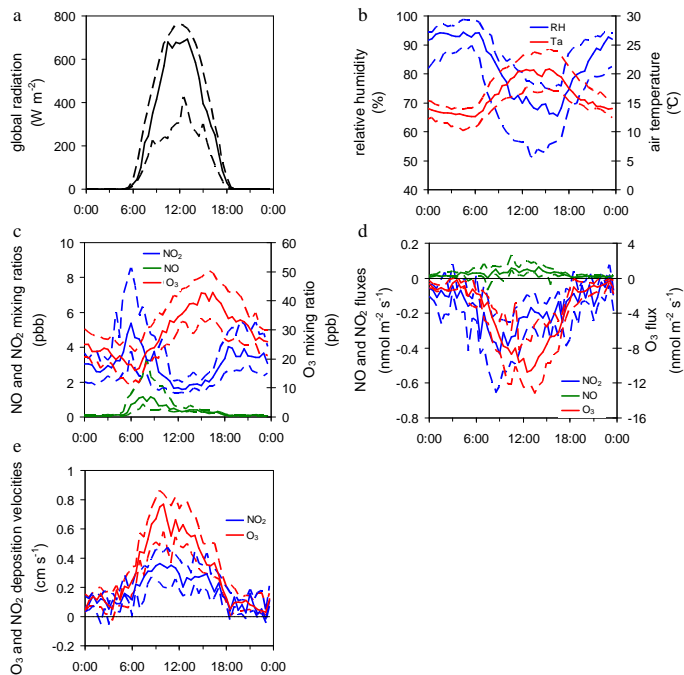


**Fig. 2.** Diel courses of **(a)** global radiation, **(b)** air relative humidity (blue line) and temperature (red line), **(c)** nitrogen dioxide (blue line), nitric oxide (green line) and ozone (red line) mixing ratios at 1.65 m above ground level, **(d)** nitrogen dioxide (blue line), nitric oxide (green line) and ozone (red line) fluxes, and **(e)** deposition velocities for nitrogen dioxide (blue line) and ozone (red line) determined by EC from 29 August to 20 September 2005. Solid lines represent half hourly medians and dotted lines represent interquartile ranges. Fluxes were not corrected for chemical reactions. Only those data have been considered, for which footprint analysis indicated that at least 95 % of the fluxes have originated from the experimental field (see Fig. 3).

Title Page

Abstract

Introduction

Conclusions

References

Tables

Figures



Back

Close

Full Screen / Esc

Printer-friendly Version

Interactive Discussion



## Measurements of nitrogen oxides and ozone fluxes

P. Stella et al.

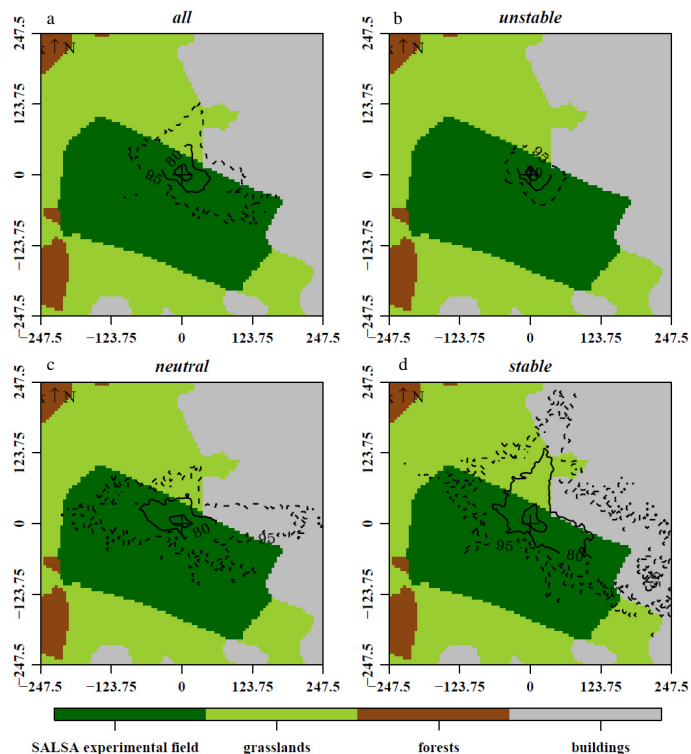


**Fig. 3.** Averaged cumulative footprint contours showing the footprint areas for 80 % (solid line) and 95 % (dotted line) of the total flux measured by eddy covariance for **(a)** all, **(b)** unstable, **(c)** neutral, and **(d)** stable conditions. x-axis and y-axis are distances from the mast (in m). The analysis was performed for all data from 29 August to 20 September 2005.

Title Page

Abstract

Introduction

Conclusions

References

Tables

Figures

◀

▶

◀

▶

Back

Close

Full Screen / Esc

Printer-friendly Version

Interactive Discussion



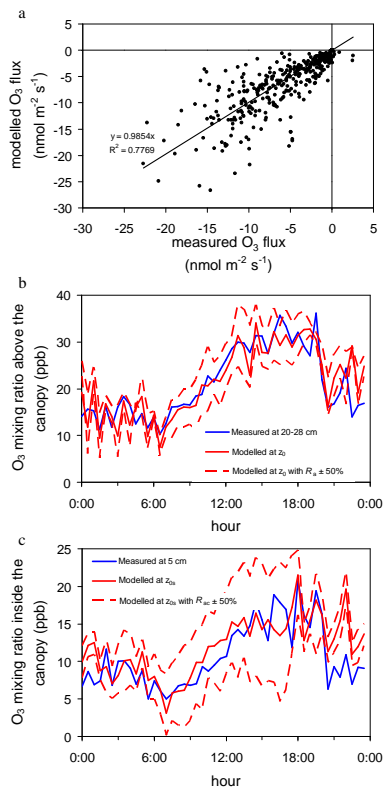


**Fig. 4.** Comparison between measured and modelled **(a)**  $O_3$  fluxes, and  $O_3$  mixing ratios **(b)** above and **(c)** within the canopy. Shown are median values from 29 August to 20 September 2005. Blue lines are measured mixing ratios, solid red lines are modelled mixing ratios and dotted red lines are modelled mixing ratios with an uncertainty of  $\pm 50\%$  for the aerodynamic resistances. For details see text.

Measurements of  
nitrogen oxides and  
ozone fluxes

P. Stella et al.

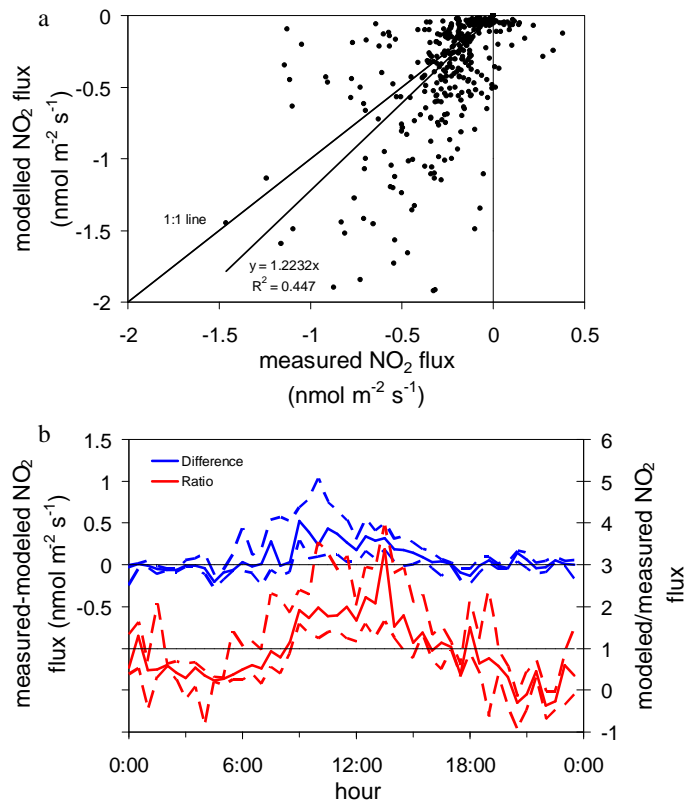


**Fig. 5.** (a) Comparison between measured and modelled NO<sub>2</sub> fluxes. (b) Half hourly median (solid lines) and interquartile range (dotted lines) of the difference (blue lines) and ratio (red lines) between measured and modelled NO<sub>2</sub> fluxes from 29 August to 20 September 2005.

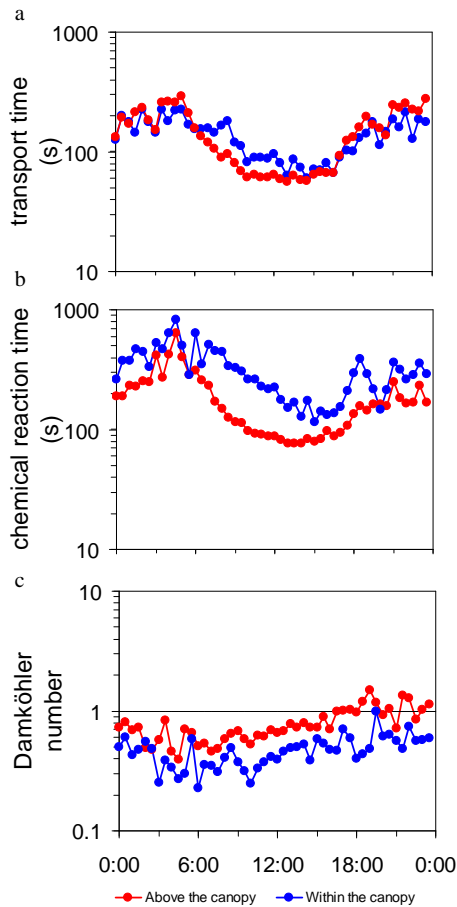


**Fig. 6.** Half hourly medians of **(a)** transport times, **(b)** chemical reaction times, and **(c)** Damköhler numbers above (red symbols) and within (blue symbols) the canopy from 29 August to 20 September 2005.

## Measurements of nitrogen oxides and ozone fluxes

P. Stella et al.

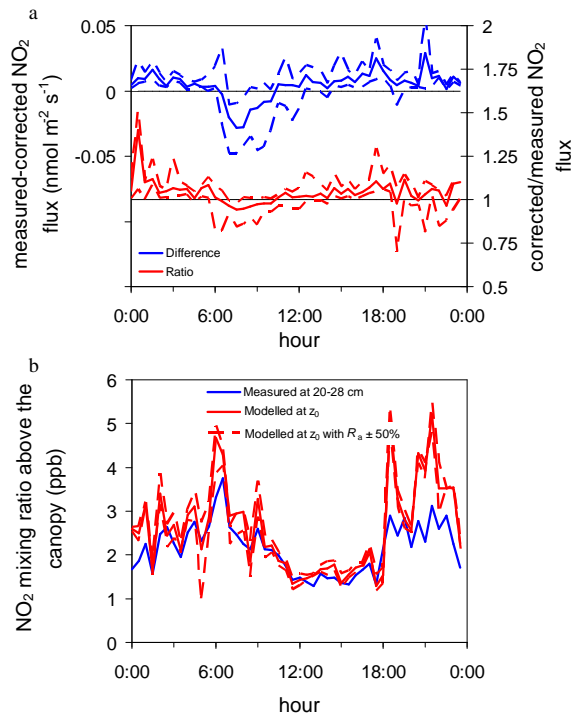


**Fig. 7.** (a) Half hourly median (solid line) and interquartile range (dotted lines) of the difference (blue lines) and the ratio (red lines) between measured NO<sub>2</sub> fluxes at  $z = 2.0$  m and NO<sub>2</sub> fluxes corrected for chemical reactions above the canopy from 29 August to 20 September 2005. (b) Comparison between measured (blue line) and modelled (red lines) NO<sub>2</sub> mixing ratio above the canopy. Dotted lines are mixing ratios modelled with an uncertainty of  $\pm 50\%$  for the aerodynamic resistance. For details see text.

[Title Page](#)
[Abstract](#)
[Introduction](#)
[Conclusions](#)
[References](#)
[Tables](#)
[Figures](#)
[Back](#)
[Close](#)
[Full Screen / Esc](#)
[Printer-friendly Version](#)
[Interactive Discussion](#)

Measurements of  
nitrogen oxides and  
ozone fluxes

P. Stella et al.

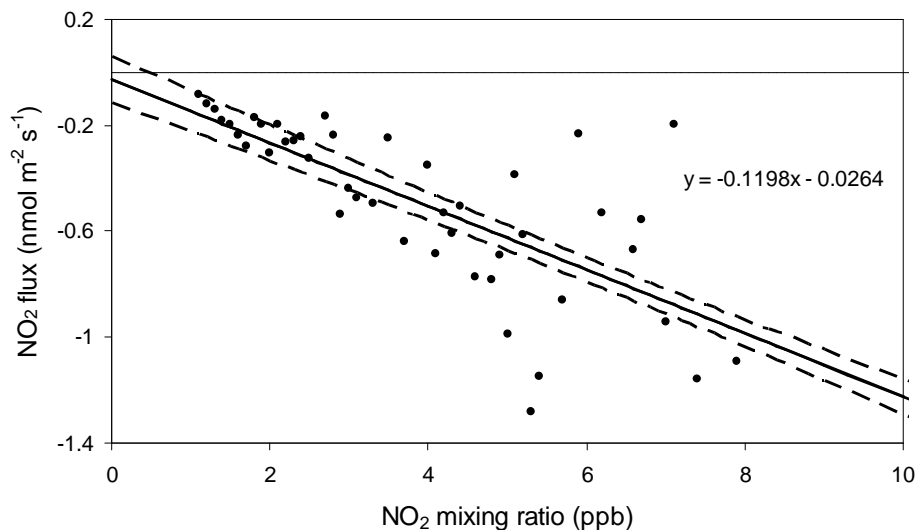


**Fig. 8.** Measured NO<sub>2</sub> flux as a function of the NO<sub>2</sub> mixing ratio ( $z = 2.0$  m) from 29 August to 20 September 2005. Solid and dotted lines are the regression line and its 95 % confidence interval, respectively. NO<sub>2</sub> fluxes were corrected for chemical reactions above the canopy and averaged for NO<sub>2</sub> mixing ratio bins of 0.1 ppb. Only data for  $G_r > 400 \text{ Wm}^{-2}$  were included.

[Title Page](#)[Abstract](#)[Introduction](#)[Conclusions](#)[References](#)[Tables](#)[Figures](#)[Back](#)[Close](#)[Full Screen / Esc](#)[Printer-friendly Version](#)[Interactive Discussion](#)

## Measurements of nitrogen oxides and ozone fluxes

P. Stella et al.

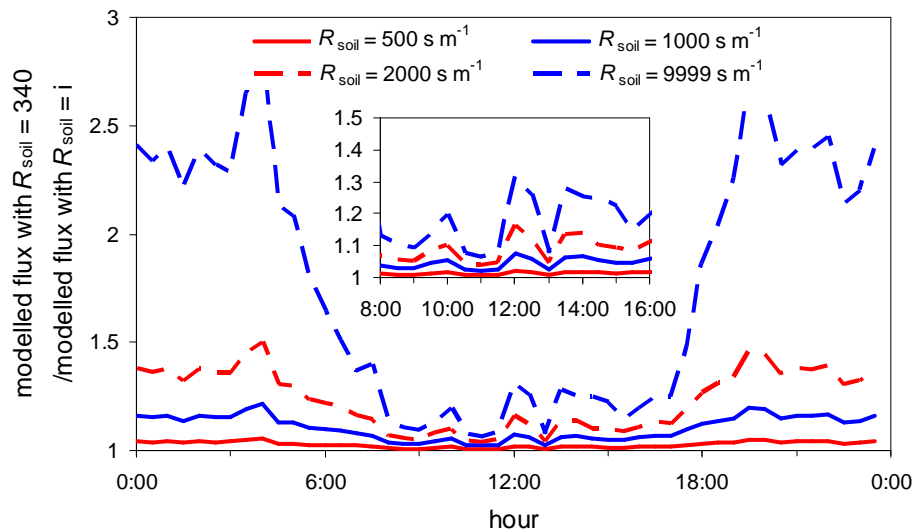


**Fig. 9.** Half hourly median of the response of the modelled  $\text{NO}_2$  deposition flux to the soil resistance for  $R_{\text{soil}}^{\text{NO}_2} = 500 \text{ s m}^{-1}$  (solid red line),  $R_{\text{soil}}^{\text{NO}_2} = 1000 \text{ s m}^{-1}$  (solid blue line),  $R_{\text{soil}}^{\text{NO}_2} = 2000 \text{ s m}^{-1}$  (dotted red line), and  $R_{\text{soil}}^{\text{NO}_2} = 9999 \text{ s m}^{-1}$  (dotted blue line) from 29 August to 20 September 2005. The reference  $\text{NO}_2$  flux was modelled using  $R_{\text{soil}}^{\text{NO}_2} = 340 \text{ s m}^{-1}$ .

Title Page

Abstract

Introduction

Conclusions

References

Tables

Figures

◀

▶

◀

▶

Back

Close

Full Screen / Esc

Printer-friendly Version

Interactive Discussion



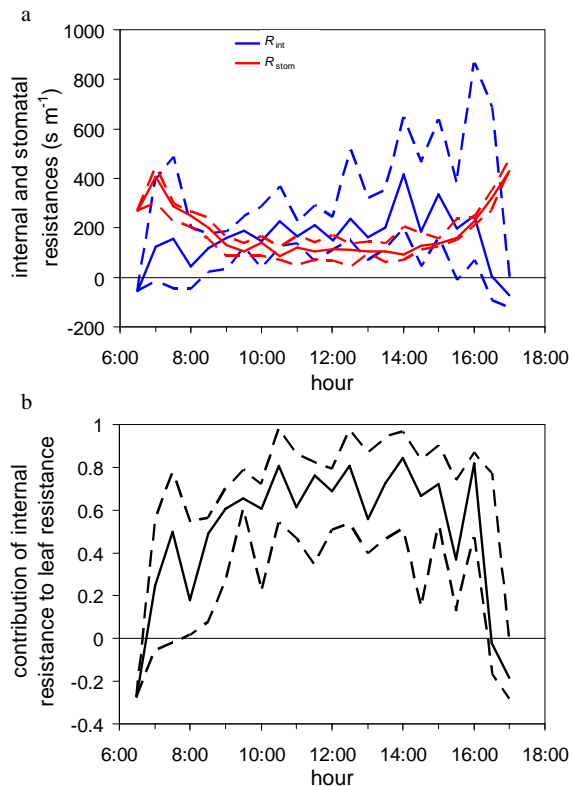


**Fig. 10.** Half hourly medians (solid lines) and interquartile range (dotted lines) of **(a)**  $\text{NO}_2$  internal (blue lines) and stomatal resistances (red lines) and **(b)** the relative contribution of internal resistance to the total leaf resistance ( i.e.  $R_{\text{int}}^{\text{NO}_2} / \left( \frac{1}{R_{\text{cut}}^{\text{NO}_2}} + \frac{1}{R_{\text{int}}^{\text{NO}_2} + R_{\text{s}}^{\text{NO}_2}} \right)^{-1}$ ) during daytime from 29 August to 20 September 2005. Only data for  $1/R_{\text{s}}^{\text{NO}_2} > 0.2 \text{ cm s}^{-1}$  ( $R_{\text{s}}^{\text{NO}_2} < 500 \text{ s m}^{-1}$ ) were included.